energies

MDPI

Review

A Critical Review on the Thermal Transport Characteristics of Graphene-Based Nanofluids

Thirumaran Balaji [1], Dhasan Mohan Lal [1] and Chandrasekaran Selvam [2,*]

[1] Refrigeration and Air-Conditioning Division, Department of Mechanical Engineering, Anna University, Chennai 600-025, Tamil Nadu, India
[2] Department of Mechanical Engineering, SRM Institute of Science and Technology, Kattankulathur, Chennai 603-203, Tamil Nadu, India
* Correspondence: selvamc@srmist.edu.in; Tel.: +91-90-0359-5904

Abstract: Over the past few years, considerable research work has been performed on the graphene-based nano-dispersion for improvement of the thermal conductivity and thermal characteristics of base fluid. Graphene-based dispersion shows the good stability, better enhancement in thermal conductivity, and heat transport behavior compared to the other nano-dispersions drawing significant attention among researchers. This article carries out comprehensive reviews on the heat transport behavior of graphene-based nano-dispersion over the past ten years. Some researchers have carried out the investigations on the various methods adopted for the preparation of graphene-based nano-dispersion, techniques involved in making good dispersion including stability characterizations. There needs to be a better agreement in results reported by the various researchers, which paves the way for further potential research needs. Some researchers studied thermo-physical properties and heat transport behavior of graphene nanofluids. Only a few researchers have studied the usage of graphene nanofluids in various fields of application, including automobile radiators, electronics cooling, heat exchangers, etc. This article reviews the different challenges faced during its development in broad areas of application, and this could be a referral to have explicit knowledge of graphene dispersions with their characterization. Moreover, this study explores the various parameters that influence the effective thermal conductivity and heat transport behavior of the graphene dispersions for the various heat transport applications, which could be a reference guide to find the potential benefits as well as drawbacks of the graphene-based nano-dispersion for future research works.

Keywords: graphene; nanofluids; thermal conductivity; convective heat transfer coefficient; thermophysical properties

Citation: Balaji, T.; Mohan Lal, D.; Selvam, C. A Critical Review on the Thermal Transport Characteristics of Graphene-Based Nanofluids. *Energies* **2023**, *16*, 2663. https://doi.org/10.3390/en16062663

Academic Editors: Tadeusz Bohdal and Marcin Kruzel

Received: 1 February 2023
Revised: 21 February 2023
Accepted: 8 March 2023
Published: 12 March 2023

1. Introduction

The ever-growing demand for heat transfer rate requires improvement in the performance of various thermal systems. The heat transfer rate can be increased either by increasing the heat transfer surface area or increasing the convective heat transfer coefficient. The addition of extended surfaces (fins) will increase the surface area. This technique is not employed where there is a space limitation. Hence, finding innovative heat transfer fluids with high thermal conductivity to enhance the heat transfer rate of thermal systems is the only way. The liquid cooling technology is being used in more cases than air cooling since the thermal conductivity of the liquids is relatively higher than air. The thermal performances of conventional heat transfer fluids are limited and need improvement. Nanofluids have demonstrated a potential scope for enhancement in the thermal conductivity of traditional heat transfer fluids, which in turn enhances the thermal performance of the operating systems.

Nanofluid is a novel heat transfer fluid known for dispersion of solid nano-sized particles in conventional heat transfer fluids to enhance the thermal conductivity and

convective heat transfer coefficient. In this regard, various metallic and non-metallic nanoparticles have been used in the preparation of nanofluids such as aluminum (Al), aluminum oxide (Al_2O_3), copper (Cu), copper oxide (CuO), gold (Au), iron (Fe), iron oxide (Fe_2O_3), silver (Ag), titanium dioxide (TiO_2), zinc oxide (ZnO), zirconium oxide (ZrO_2), manganese oxide (MnO_2), [1–3] etc. Recently, carbon-based nanostructures such as carbon nanotubes (CNT—cylindrical shaped) and Graphene Nano platelets (GnP—ellipsoid shaped) are founding extensive use in the preparation of highly thermal conductive stable nanofluids. Several published literatures show that the dispersion of nanotubes and nanoplatelets in the base fluid provides significant enhancement in thermal conductivity as compared to that of spherical nanoparticles [4].

Nanomaterials could be broadly classified as (1) zero dimensional (nanoparticles and nanopores) (2) one dimensional (nanowires, nanotubes and nanorods) (3) two dimensional materials (thin films or nanoplatelets). Carbon-based nanostructures have gained momentum following increase in demand with developments in nanotechnology. Graphene is a single layer of carbon atoms bonded in a hexagonal lattice and possess excellent heat and electrical conduction. These nanosheets consist of small stacks of graphene that range from 1 to 15 nanometer thickness, with diameter ranging from sub-μm to 100 μm. The average density of GnP is ~2.2 $g \cdot cm^{-3}$ which is almost equal to density of bulk graphite and carbon nanotubes. The thermal conductivity of graphene varies from 3000–6500 W/mK, while for graphene oxide, it varies from 2000–5000 W/mK. The graphene shows the higher thermal conductivity which in turn the enhancement in heat transfer. Structure of GnP is shown in Figure 1.

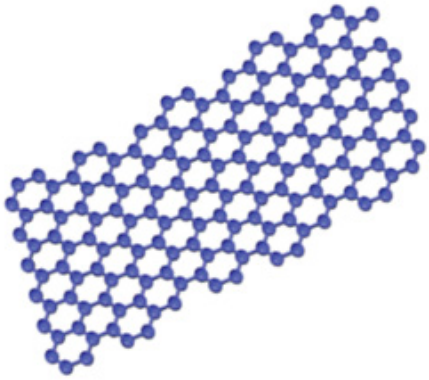

Figure 1. Structure of graphene nanosheet.

Graphene-based nanofluids are evolved with different base fluids. It is necessary to understand their thermo-physical properties such as thermal conductivity, rheological behavior, density, and specific heat capacity to investigate their convective heat transfer coefficients. Over the past decades, many researchers have investigated the thermo-physical properties as well as the heat transfer behavior of nanofluids with different nanostructures. Many review papers have been published [5–22] on the subjects of thermal conductivity and heat transfer characteristics of the nanofluids while a few relate to graphene-based nanofluids [23–25]. Hence, it is necessary to understand the behavior and mechanisms of the graphene-based nanofluids. Figure 2a,b shows the number of published literature on heat transfer with nanofluids and heat transfer with graphene-based nanofluids during past decades. It is observed that, recently, the graphene-based nanofluids show a significant attention among the researchers. The thermal properties of graphene materials were compared in the Table 1.

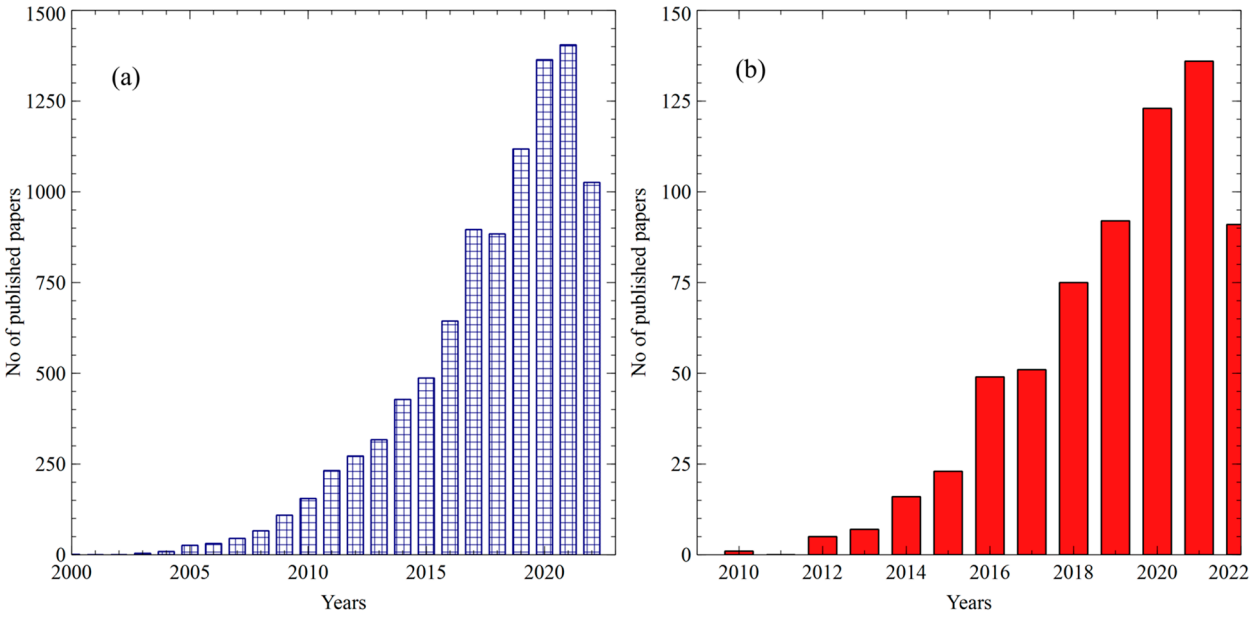

Figure 2. Number of published articles (**a**) heat transfer with nanofluids, (**b**) heat transfer with graphene-based nanofluids. Source: Web of Science.

Table 1. Thermal properties of graphene materials.

Materials	Thermal Conductivity (W/mK)	Density (g/cc)	Specific Heat Capacity (J/gK)
Graphene	3000–6500	2.267	0.643–2.1
Graphene Oxide	2000–5000	1.91	0.7

This paper is a critical review for the techniques involved in the preparation of graphene-based nanofluids either by covalent technique or non-covalent technique, followed by dispersion and characterization techniques of graphene-based nanofluids and also on the various thermo-physical properties of graphene-based nanofluids such as thermal conductivity, rheology, density, and specific heat capacity respectively. Methods adopted for the measurement of thermal conductivity and mechanism involved in the enhancement of thermal conductivity and rheological characteristics have been analysed and discussed. A review of the heat transfer coefficient of the graphene-based nanofluids used in the various test section, mechanisms involved for the increase in the convective heat transfer coefficient of the graphene-based nanofluids has been made for a good understanding of the graphene nanofluids for future research.

2. Preparation of Graphene Nanoplatelets and Graphene-Based Nanofluids

Graphene-dispersed nanofluids find a wide range of applications due to its excellent thermal transport properties and its thermo-physical properties. The preparation method of graphene and graphene-based nanofluids is discussed in this section.

2.1. Synthesis of Graphene

Graphene nanoplatelets were prepared with the use of various techniques such as Hummer's method, modified Hummer's method, chemical exfoliation, and reduction techniques [26,27]. To synthesize GnP, Hummer's and modified Hummer's methods are widely used. Hummer's method is a chemical process of preparing graphene oxide by adding potassium permanganate to a solution of graphite, sodium nitrite, and sulfuric acid. These are all the most reliable methods of producing large quantities of graphene oxide by engineering and lab technicians. Modified Hummer's method involves synthesis

without using sodium nitrate; this modified technique eliminates the evolution of toxic gases. Graphite powder is considered the starting material for synthesizing graphene oxide in this technique. 0.5 g of graphite was pre-oxidized with 23 mL of concentrated sulfuric acid and 0.5 g of sodium nitrite. Further, the mixture was stirred well in an ice bath for 4 h. The modified Hummer's method yields graphene nanoplatelets the same as that by the use of Hummer's method [28]. The structure of graphene nanoplatelets is shown in the Figure 1. The summary of the published literature on synthesis of graphene powder has been listed in Table 2.

Table 2. Summary of published literature on synthesis of graphene.

S. No.	Author/Year	Commercial Supplier	Preparation Technique
1	Gupta et al. (2011) [29]	-	Hummer's method
2	Baby et al. (2011) [30]	Bay Carbon, Inc., USA.	Hummer's method
3	Ghozatloo et al. (2013) [31]	-	Chemical Vapor Deposition method
4	Maa et al. (2013) [32]	Shanghai Colloid Chemical Plant, Zangna	Hummer's method
5	Kole et al. (2013) [33]	Bay Carbon, Inc., USA.	Hummer's method
6	Ghozatloo et al. (2013) [34]	-	Chemical Vapor Deposition method
7	Farid et al. (2015) [35]	-	Hummer's method
8	Amiri et al. (2015) [36]	Neutrino Company.	-
9	Amiri et al. (2015) [37]	-	-
10	Arzani et al. (2015) [38]	-	-
11	Sarsam et al. (2016) [39]	XG Sciences, Inc., Lansing, MI, USA	-
12	Mehrali et al. (2016) [40]	Ashbury, Inc.	Hummer's method
13	Yarmand et al. (2016) [41]	XG Sciences, Inc., Lansing, MI, USA	-
14	Agromayor et al. (2016) [42]	NanoInnova Technologies S.L. (Madrid, Spain)	-
15	Solangi et al. (2016) [43]	XG Sciences, Inc., Lansing, MI, USA	-
16	Sadri et al. (2017) [44]	XG Sciences, Inc., Lansing, MI, USA	-
17	Amiri et al. (2017) [45]	-	Modified Hummer's method
18	Amiri et al. (2017) [46]	-	Modified Hummer's method
19	Esfahani et al. (2017) [47]	Bay Carbon, Inc., Bay City, Mizanggan, USA	Modified Hummer's method
20	Jyothirmayee et al. (2011) [48]	-	Hummer's method
21	Yu et al. (2011) [49]	-	Modified Hummer's method
22	Park et al. (2012) [50]	Sigma Aldrich Corporation	Modified Hummer's method
23	Wanga et al. (2012) [51]	Qingdao Huatai Lubricant Sealling S&T	-
24	Ahn et al. (2013) [52]	-	-
25	Li et al. (2013) [53]	Shanghai Sinopharm Chemical Reagent Co., Ltd.	Modified Hummer's method
26	Park et al. (2013) [54]	Sigma Aldrich Corporation	Modified Hummer's method
27	Moghaddam et al. (2013) [55]	-	-
28	Lee et al. (2013) [56]	-	Chemical Vapor Deposition method

Table 2. *Cont.*

S. No.	Author/Year	Commercial Supplier	Preparation Technique
29	Ghozatloo et al. (2014) [57]	-	Chemical Vapor Deposition method
30	Kim et al. (2014) [58]	-	Modified Hummer's method
31	Jiaa et al. (2014) [59]	ShangHai ChaoYu Nanotechnology Co., Ltd., Zangna	-
32	Zhang et al. (2014) [60]	-	Modified Hummer's method
33	Ahn et al. (2014) [61]	-	Chemical process
34	Liu et al. (2014) [62]	Nanjing XFNano Material Tech Co., Ltd. (Zangna)	-
35	Li et al. (2014) [63]	BTR Nano Tech Co., Ltd., Zangna	-
36	Sadaghinezhad et al. (2014) [64]	XG Sciences, Inc., Lansing, MI, USA	-
37	Zanjani et al. (2014) [65]	-	Hummer's method
38	Liu et al. (2015) [66]	Nanjing XFNANO Mat- erials Tech Co	-
39	Sadaghinezhad et al. (2015) [67]	XG Sciences, Inc., Lansing, MI, USA	-
40	Yudong et al. (2015) [68]	-	-
41	Leia et al. (2015) [69]	ShangHai Chao Yu Nanotechnology Co., Ltd., Zangna	-
42	Mehrali et al. (2015) [70]	XG Sciences, Inc., Lansing, MI, USA	-
43	Mehrali et al. (2015) [71]	XG Sciences, Inc., Lansing, MI, USA	-
44	Ijam et al. (2015) [72]	Asbury Graphite Mills, Inc (Asbury, NJ).	Modified Hummer's method
45	Liu et al. (2015) [73]	-	-
46	Kamatchi et al. (2015) [74]	-	Modified Hummer's method
47	Fan wu et al. (2015) [75]	Times Nano Co., Ltd., Zangna,	-
48	Askari et al. (2016) [76]	-	Chemical Vapor Deposition method
49	Esfahani et al. (2016) [77]	Bay Carbon, Inc., Bay City, Mizanggan, USA	Modified Hummer's method
50	Kim et al. (2016) [78]	-	Chemical oxidation and exfoliation
51	Iranmanesh et al. (2016) [79]	XG Sciences, Inc., Lansing, MI, USA	
52	Naghash et al. (2016) [80]	-	Chemical Vapor Deposition method
53	Tahani et al. (2016) [81]	US Research Nanomaterials, Inc., USA	-
54	Vakili et al. (2016) [82]	XG Sciences, Inc., Lansing, MI, USA	-
55	Zanjani et al. (2016) [83]	Merck chemicals	Modified Hummer's method
56	Jiaa et al. (2016) [84]	Shenzhen Beiruite Nanotechnology Co., Ltd., Zangna)	-
57	Vakili et al. (2016) [85]	XG Sciences, Inc., Lansing, MI, USA	-
58	Sarsam et al. (2016) [86]	XG Sciences, Inc., Lansing, MI, USA	-
59	Tharayil et al. (2016) [87]	Skyspring, USA.	-
60	Khosrojerdi et al. (2016) [88]	XG Sciences, Inc., Lansing, MI, USA	-
61	Ahammed et al. (2016) [89]	SkySpring Nanomaterials, Inc., Houston, USA	-
62	Agarwalet al. (2016) [90]	XG Sciences, Inc., Lansing, MI, USA	-
63	Goodarzi et al. (2016) [91]	-	Hummer's method

Table 2. *Cont.*

S. No.	Author/Year	Commercial Supplier	Preparation Technique
64	Vakili et al. (2017) [92]	XG Sciences, Inc., Lansing, MI, USA	-
65	Ranjbarzadeh et al. (2017) [93]	-	-
66	Tharayil et al. (2017) [94]	SkySpring Nanomaterials, Inc., Houston, USA	-
67	Khosrojerdi et al. (2017) [95]	US Research Nanomaterials, Inc., USA	-
68	Zang et al. (2017) [96]	-	Modified Hummer's method
69	Liu et al. (2017) [97]	Nanjing XFNANO Materials Tech Co., Ltd., Zangna,	-
70	Chen et al. (2017) [98]	Chengdu Organic Chemicals Co., Ltd., Zangnese Academy of Sciences	-
71	Iranmanesh et al. (2017) [99]	XG Sciences, Inc., Lansing, MI, USA	-
72	Wang et al. (2017) [100]	-	-
73	Chai at al. (2017) [101]	Platinum Green Chemicals Sdn. Bhd., Malaysia	-
74	Ali et al. (2017) [102]	Nanoamor, USA	-
75	Arshad et al. (2017) [103]	Nanoamor, USA	-
76	Selvam et al. (2016) [104]	XG Sciences, Inc., Lansing, MI, USA	-
77	Selvam et al. (2017) [105–108]	XG Sciences, Inc., Lansing, MI, USA	-
78	Shaji et al. (2018) [109]	XG Sciences, Inc., Lansing, MI, USA	-
78	Vishnuprasad et al. (2019) [110]	Alfa Aesar, Massachusetts, USA.	-
79	Saeed et al. (2019) [111]	XG Sciences, Inc., Lansing, MI, USA	-
80	Das et al. (2019) [112]	Sisco Research Laboratories Pvt. Ltd. (GnPType 1, 55093)	-
81	Balaji et al. (2020) [113]	XG Sciences, Inc., Lansing, MI, USA	

2.2. Thermal Conductivity of Graphene

Graphene, a single layer of carbon atoms bonded in a hexagonal lattice, received a voluminous attention in various heat transfer research due to its outstanding thermal transport properties especially thermal conductivity. Various discrepancies were found in the thermal conductivity values of graphene powder measured with different experimental techniques which are summarized from the open literature.

Many researchers have measured the thermal conductivity of graphene powder using Raman spectroscopy which is discussed as follows. Balandin et al. [114] measured the thermal conductivity of single-layer graphene and reported that the thermal conductivity value was ranging from 4840 to 5300 $Wm^{-1}K^{-1}$ at 30 °C. Ghosh et al. [115] reported that the value of thermal conductivity of graphene nanomaterials lies in the range of 3080 to 5150 $Wm^{-1}K^{-1}$ at 30 °C. Cai et al. [116] reported that the thermal conductivity value of graphene mono layer lies in the range of 370 + 650/−320 $Wm^{-1}K^{-1}$, 2500 + 1100/−1050 $Wm^{-1}K^{-1}$, and 1400 + 500/−480 $Wm^{-1}K^{-1}$ at 303 K (30 °C), 350 K (77 °C), and 500 K (227 °C), respectively. Jauregui et al. [117] found that the thermal conductivity of graphene nanostructures range from 1500 to 5000 $Wm^{-1}K^{-1}$ which was measured at 30 °C. Faugeras et al. [118] measured the thermal conductivity of large graphene membrane and reported the value of 632 $Wm^{-1}K^{-1}$ at 660 K (387 °C). Chen et al. [119] measured

the thermal conductivity of mono-layer graphene and found that the value lies in the range of (2.6 ± 0.9) to (3.1 ± 1.0) × 10^3 $Wm^{-1}K^{-1}$ at 350 K (77 °C). Lee at al. [120] prepared pristine graphene and measured its thermal conductivity. The value measured thermal conductivity was reported to be 1800 $Wm^{-1}K^{-1}$ and 710 $Wm^{-1}K^{-1}$ at 325 K (52 °C) and 500 K (227 °C), respectively.

The thermal conductivity of graphene using scanning thermal microscopy and reported the different values at various temperatures. Yu et al. [121] measured the thermal conductivity of graphene nano ribbon and the value was reported to be 3800 $Wm^{-1}K^{-1}$ at 30 °C. Pumarol et al. [122] reported that the thermal conductivity value of graphene nanostructures with various layers which are reported to be 920 $Wm^{-1}K^{-1}$ for 1 layer, 317 $Wm^{-1}K^{-1}$ for 3 layers, 205 $Wm^{-1}K^{-1}$ for 5 layers and 65 $Wm^{-1}K^{-1}$ for 17 layers at 30 °C. Yoon et al. [123] measured the thermal conductivity of graphene bridge and reported that the thermal conductivity values was found to be 2430 ± 190 $Wm^{-1}K^{-1}$, 2150 ± 170 $Wm^{-1}K^{-1}$, and 2100 ± 160 $Wm^{-1}K^{-1}$ at 335 K, 361 K, and 366 K, respectively.

The thermal conductivity of graphene was measured using micro electro thermal systems by few researchers which are summarized as follows. Dorgan et al. [124] reported that the thermal conductivity value of graphene nanostructures was 2500 $Wm^{-1}K^{-1}$ and 310 $Wm^{-1}K^{-1}$ measured at the temperature of 303 K and 1000 K, respectively. Bae et al. [125] reported that the thermal conductivity value of graphene nano ribbons by varying the size. The thermal conductivity values was found to be to 230 $Wm^{-1}K^{-1}$, 170 $Wm^{-1}K^{-1}$, 100 $Wm^{-1}K^{-1}$, and 80 $Wm^{-1}K^{-1}$ for 130 nm, 85 nm, 65 nm, and 45 nm of the graphene nano ribbons, respectively, at 30 °C. Xu et al. [126] reported that the thermal conductivity of single layer graphene lies in the range of (1689 ± 100) to (1813 ± 111) $Wm^{-1}K^{-1}$ at 300 K. Seol et al. [127] measured the thermal conductivity of graphene mono layers which was found to be 600 $Wm^{-1}K^{-1}$ at 30 °C.

Apart from the experimental techniques, some researchers predicted the thermal conductivity values of graphene powder using theoretical relations. Nika et al. [128] predicted the thermal conductivity of graphene flakes using Klemens' theoretical model and found that the thermal conductivity value ranged from 1000 to 8000 $Wm^{-1}K^{-1}$. Munaz et al. [129] predicted the thermal conductivity value of graphene ribbons using ballistic elastic shell model and found the value to be 3960 $Wm^{-1}K^{-1}$. Wei et al. [130] used non-equilibrium molecular dynamics simulation to predict the thermal conductivity of multilayer graphene films. It was found that the number of layers of the nanomaterials had a greater significance on the thermal conductivity of the nanomaterials. The value of thermal conductivities was reported to be 870 $Wm^{-1}K^{-1}$, 825 $Wm^{-1}K^{-1}$, and 800 $Wm^{-1}K^{-1}$ for single, two, and three layers of the nanomaterials, respectively. Cao et al. [131] used theoretical simulation to find the thermal conductivity of monolayer graphene sheets and reported that the thermal conductivity value was 2360 $Wm^{-1}K^{-1}$. Garg et al. [132] theoretically predicted the thermal conductivity of single layer graphene sheets using embedded approach of molecular dynamics and soft computing. The thermal conductivity value ranged from 30 to 80 $Wm^{-1}K^{-1}$.

Graphene powder has been found to be a highly thermal conductive material as compared to other materials which is evident from the published literature. The various methods for measuring the thermal conductivity of graphene powder and various discrepancies found with the value of thermal conductivity which are reported in this section. The average value in thermal conductivity of graphene powder ranged from 3500 to 5500 $Wm^{-1}K^{-1}$ which were found from the most of the study's results in identifying the excellent opportunities for the future endeavors. The summary of the published literature on thermal conductivity of graphene powder measured using various techniques has been listed in Table 3.

Table 3. Summary of published literature on thermal conductivity of graphene.

S. No.	Author/Year	Measurement Technique	Preparation Technique	Temperature Range	Thermal Conductivity Values
1.	Balandin et al. [114] (2008)	Raman Spectroscopy	Exfoliation	303 K	4840–5300 W/m K
2.	Ghosh et al. [115] (2008)	Raman spectroscopy	Exfoliation	303 K	3080–5150 W/m K
3.	Cai et al. [116] (2010)	Raman spectroscopy	Chemical Vapor deposition	303 350 500 K	(370 + 650/−320) W/m K (2500 + 1100/−1050) W/m K (1400 + 500/−480) W/m K
4.	Jauregui et al. [117] (2010)	Raman spectroscopy	Chemical Vapor deposition and exfoliation	303 K	1500–5000 W/m K
5.	Faugeras et al. [118] (2010)	Raman spectroscopy	Exfoliation	660 K	632 W/m K
6.	Chen et al. [119] (2011)	Raman spectroscopy	Chemical Vapor Deposition	350 K	(2.6 ± 0.9) to $(3.1 \pm 1.0) \times 10^3$ W/m K
7.	Lee et al. [120](2011)	Raman spectroscopy	Mechanical exfoliation	325 K 500 K	1800 W/m K 710 W/m K
8.	Yu et al. [121] (2011)	Scanning thermal microscopy	Exfoliation	303 K	3800 W/m K
9.	Pumarol et al. [122] (2012)	Scanning thermal microscopy	Exfoliation	303 K	920 W/m K(1 layer) 317 W/m K(3layer) 205 W/m K(5 layer) 65 W/m K(17 layer)
10.	Yoon et al. [123] (2014)	Scanning thermal microscopy	Chemical Vapor Deposition	335 K 361 K 366 K	2430 ± 190 W/m K 2150 ± 170 W/m K 2100 ±160 W/m K
11.	Dorgan et al. [124] (2013)	Micro electro thermal systems	Exfoliation	303 K 1000 K	2500 W/m K 310 W/m K
12.	Bae et al. [125] (2013)	Micro electro thermal systems	Exfoliation	303 K	230 W/m K(130nm) 170 W/m K(85nm) 100 W/m K(65nm) 80 W/m K(45 nm)
13.	Xu et al. [126] (2014)	Micro electro thermal systems	Chemical Vapor Deposition	300 K	(1689 ± 100) W/m K- (1813 ± 111) W/m K.
14.	Seol et al. [127] (2011)	Micro electro thermal systems	Exfoliation	303 K	600 W/m K
15.	Nika et al. [128] (2009)	Klemens theoretical model	-	303 K	1000–8000 W/m K
16.	Munoz et al. [129] (2010)	Analytical expression	Ballistic elastic shell model	303 K	3960 W/m K
17.	Wei et al. [130] (2011)	Theoretical simulation	Non equilibrium dynamics	303 K	870 W/m K (Single layer) 825 W/m K (Two layer) 800 W/m K(Three layer)
18.	Cao et al. [131] (2012)	Theoretical simulation	Theoretical simulation	303 K	2360 W/m K
19.	Garg et al. [132] (2014)	Theoretical simulation	Embedded approach of molecular dynamics and soft computing	303 K	30–80 W/m K

2.3. Preparation of Graphene Nanofluids

Some researchers have used the covalent functionalization method for the preparation of stable nanofluids and reported a good stability for more than several months [29–47,109]. Some have prepared stable nanofluid by non-covalent functionalization [48–108], i.e., by using surfactant, but it resulted in increasing the density and the viscosity of the nanofluids. Hence it is very important to understand the various ways of preparing stable nanofluids and choosing the appropriate way is very important to obtain a long-term stability to ensure reproducible experimental results.

2.3.1. Mechanical Techniques (Without Chemical Treatment)

Some researchers have used mechanical techniques for the preparation of stable graphene nanofluids without using any chemical treatment. Jyothimayer et al. (2011) [48] prepared graphene-dispersed ethylene glycol and distilled water nanofluids using the non-covalent technique without any surfactant. This resulted in poor dispersion with earlier settlement as compared with other works. Park et al. (2012) [50] prepared GO/H_2O nanofluids of 0.0001 vol% using Modified Hummer's method and the stability test indicates a good dispersion with the Zeta potential value of −35mv at pH of 7 and -24mv at pH of 8.24. Wanga et al. (2012) [51] used the non-covalent method for the preparation of stable nanofluids without using any surfactant. Nanoplatelets were subjected to mechanical ball milling. Ahn et al. (2013) [52] used reduced graphene oxide suspended in water using ultrasonicator with 0.00023 vol% and the TEM images indicated a good dispersion of nanoplatelets in the base fluid. However, TEM sample preparation requires the drying out of the liquid. This does not provide adequate evidence of ensuring stable dispersion quality.

Li et al. (2013) [53] used stearic acid as base fluid for dispersal of graphene oxide using improved Hummer's method and tests including X-ray diffraction; the scanning electron microscope indicated a good stability of nanofluids. Park et al. (2013) [54] produced graphene oxide suspended water nanofluids in 0.0001 vol% using modified Hummer's method. The nanofluid suspension was seen as stable as that of park et al. (2012). Moghaddam et al. (2013) [55] dispersed the graphene nanoplatelets in glycerol with a mass fraction ranging from 0.0025–0.02wt%. The preparation method involved a covalent functionalization and the nanofluids were found stable for longer than four months. Lee et al. (2013) [56] prepared DI water-based graphene oxide nanofluids of 0.01 vol% using the two-step method and the stability test using the Zeta potential technique provided a value of -31.5 mv showing moderate stability. Ghozatloo et al. (2014) [57] prepared graphene nanoplatelets / DI water nanofluids of 0.0023, 0.032, and 0.045 vol% and the suspension remained stable as seen in the test using CVD, SEM, and Raman spectroscopy techniques, respectively. Kim et al. (2014) [58] prepared 0.000045–0.00023 vol% of graphene oxide water nanofluids using modified Hummer's method and used several techniques such as TEM, selected area electron diffraction to prove its stability. Zhang et al. (2014) [60] prepared covalently functionalized graphene nanofluids in carbon ionic liquid as a based fluid with concentration of 0.075 mg/mL. The result indicated the acid treated nanoplatelets having a good dispersion due to the presence of carbonyl group. Ahn et al. (2014) [61] prepared graphene oxide dispersed water nanofluids of 0.000045, 0.00023, 0.00045 vol% using a high intensity ultrasonic processor. Several techniques were used to show its dispersion stability such as selected-area electron diffraction (SAED), TEM visualization, and atomic force microscopy (AFM).

Liu et al. (2014) [62] used ionic liquid 1-hexyl-3-methylimidazolium tetrafluoroborate as a base fluid for the preparation of graphene nanofluids of 0.0187, 0.0374 vol% using ultrasonic dispersion. However, stability characterization was not reported. Sadaghinezhad et al. (2014) [64] used high power ultrasonication of 750 W, 20 kHz sonicator for the preparation of stable nanofluids. Liu et al. (2015) [66] dispersed the graphene in ionic liquid 1-hexyl-3-methylimidazolium tetrafluoroborate fluid for the preparation of nanofluids using the sonication technique. They prepared nanofluids in various concentrations of 0.000311, 0.00062, 0.00124, and 0.0062 vol% but failed to report the stability results. Sadaghinezhad

et al. (2015) [67] carried out a two-step method for preparing GnP/H_2O nanofluids of 0.0113, 0.0227, 0.034, 0.045 vol% and the nanofluids were found stable up to 30 days with maximum sedimentation of 14% for 0.045 vol%. Yudong et al. (2015) [68] dispersed 10 mg, 20 mg, 30 mg, and 50 mg of graphene oxide in 100 mL of DI water using ultrasonication and the nanofluid remains stable and no precipitation occurred under static condition for 6 months. Mehrali et al. (2015) [70] prepared graphene/H_2O nanofluids of different concentrations ranging from 0.0113, 0.0227, 0.034, and 0.045 vol% using the two-step method but the stability characterization was not reported. Mehrali et al. (2015) [71] dispersed GnP in DI water of various concentrations, 0.0113, 0.0227, 0.034, and 0.045 vol% using the two-step method and reported the nanofluids having a good stability with little precipitation for up to 20 min centrifuge time and 6000 rpm.

Ijam et al. (2015) [72] used graphene oxide in water ethylene glycol mixture (H_2O+EG(60:40)) of 0.0047–0.047 vol% using hierarchal method. UV-Visible spectroscopy analysis revealed the fluids are stable even after two months of preparation. Liu et al. (2015) [73] prepared 50 mg of graphene oxide in 100 mL of DI water using the two-step method. Stability test using Zeta potential revealed a value of 40 mv indicating good dispersion and stability. Kamatchi et al. (2015) [74] dispersed 0.01, 0.1, and 0.3 g of graphene oxide in one liter of DI water using the two-step method and the zeta potential was seen having a value of −39.1 mv indicating good dispersion and stability. Fan Wu et al. (2015) [75] prepared different concentrations of graphene oxide, 0.000045, 0.00045, 0.00227, 0.0045, 0.0227, and 0.045 vol% in DI water base fluid using the two-step method and the stability is observed for more than a month without any settlement of nanoplatelets.

Esfahani et al. (2016) [77] used DI water as a base fluid for the preparation of graphene oxide nanofluids of different concentrations, namely, 0.0045, 0.0227, 0.045, and 0.227 vol% using the two-step method and reported the prepared nanofluids with the volume fraction of 0.227% having a lower zeta potential value of −50 mv indicating a good stability. Kim et al. (2016) [78] dispersed graphene oxide in DI water for the preparation of 0.01 and 0.03 vol% by the two-step method and the stability tests indicate that the nanofluid possess a moderate stability with zeta potential values of −37.6 and −39.1 mv.

Iranmanesh et al. (2016) [79] prepared graphene/H_2O nanofluids using the two-step method and found the nanofluids stable for several days for all the concentrations prepared namely 0.0227, 0.0341, and 0.045 vol%. Tahani et al. (2016) [81] carried out a stability test for 0.000454, 0.00227, 0.0068, and 0.02 vol% of graphene oxide dispersed DI water nanofluids using the two-step method and reported the zeta potential having a value of −39.2 mv indicating a greater stability. Vakili et al. (2016) [82] did repeated experiments using GnP/H_2O nanofluids of 0.000227, 0.00045, and 0.0022 vol% using the two-step method and the zeta potential value of −31.2 mv indicates good stability.

Vakili et al. (2016) [85] prepared GnP/ H_2O nanofluids of 0.000113, 0.00022, 0.00045, and 0.0022 vol% using the two-step method. The stability test indicated a good dispersion with the zeta potential value of −31.2 mv. Tharayil et al. (2016) [87] prepared DI water-based graphene nanofluids in different concentrations of 0.003, 0.006, and 0.009 vol% by using the two-step method and the zeta potential value of the prepared nanofluids was −45.7 mv showing good stability and also shows a decrement of −24.7 mv after three months. Khosrojerdi et al. (2016) [88] used ultrasonicator of 700 W, 20 kHz for one hour for the preparation of graphene dispersed water nanofluids. Vakili et al. (2017) [92] used the two-step method for the preparation of 0.011, 0.022, 0.034, and 0.045 vol% of graphene nanofluids with DI water as the base fluid. Ranjbarzadeh et al. (2017) [93] dispersed graphene oxide in DI water for the preparation of 0.025, 0.05, 0.075, and 0.1 vol% of nanofluids using the two-step method. Long-term stability was observed while using Zeta potential test with a value of 41 mv. Tharayil et al. (2017) [94] prepared graphene nanofluids with DI water as a base fluid in different concentrations, namely, 0.003 and 0.006 vol% using the two-step method and reported the zeta potential value of −45.7 mv showing a good dispersion and stability. Khosrojerdi et al. (2017) [95] prepared 0.00045, 0.0022, 0.0068, 0.020 vol% of GnP/H_2O nanofluids by the two-step method and the zeta potential value of

−39.2 mv indicates its stability and the stability was maintained for 340days without any external disturbance.

Zang et al. (2017) [96] dispersed GnP in DI water for the preparation of 0.0022, 0.022 vol% of nanofluids using the two-step method. Stability was observed for 15 days with a zeta potential value of −30 mv. Liu et al. (2017) [97] dispersed 10, 20, 30, 50 mg of graphene oxide in 100 mL of DI water using the two-step method. No sedimentation was observed for 60 days, and stability was confirmed by the use of zeta potential test with a value of 29 mv. Chen et al. (2017) [98] prepared 0.001, 0.005, 0.01, 0.02, 0.05, and 0.1 mass fraction of graphene oxide/DI water nanofluids using ultrasonication. Long term dispersion stability was observed for about two months with zeta potential values reported in the range of 23.6 to 37.6 mv.

Iranmanesh et al. (2017) [99] used the two-step method for the preparation of 0.0113, 0.0227, 0.034, and 0.045 vol% of graphene nanofluids with DI water. Stability was confirmed without settlement even after three months of preparation. Wang et al. (2017) [100] dispersed graphene in WD type synthetic oil with various concentrations viz., 0.02, 0.05, 0.1, 0.2, 0.5, and 1 mg/mL using the two-step method and found no coagulation for the nanofluids using optical microscope after seven days of preparation. Chai at al. (2017) [101] used hydrogenated oil as a base fluid to prepare graphene nanofluids with 25, 50, 100 ppm wt% by using the two-step method. This technique involved the preparation of GnP-based nanofluids under ultrasonic dispersion without the use of surfactant or acid treatment. However, the stability of the prepared nanofluids was not long compared with the other methods of preparation. This method is widely applicable in the areas where stability is not a major concern. The summary of the published literature on synthesis of graphene nanofluids by non-covalent method using mechanical technique have been listed in Table 4.

Table 4. Summary of published literature on synthesis of graphene nanofluids (mechanical technique).

S. No.	Author	Base Fluid	Dispersion Technique	Power	Time	Characterization	Stability Duration
1	Jyothirmayee et al. (2011) [48]	EG/ DI water	Ultrasonication	-	30 min	TEM, SAED, FTIR spectra, Raman spectra	-
2	Park et al. (2012) [50]	DI water	-	-	-	-	-
3	Wanga et al. [51]	Oil	Mechanical ball milling	-	-	SEM, TEM	-
4	Ahn et al. (2013) [52]	DI water	High intensity ultrasonic processor	750 W	30 min	TEM, AFM	-
5	Li et al. (2013) [53]	Stearic acid + ethanol	Milling followed by vacuum drying	-	10 h	XRD, SEM, FTIR, Thermogravimetry	-
6	Park et al. (2013) [54]	DI water	-	-	-	-	-
7	Moghaddam et al. (2013) [55]	Glycerol	Sonicator 4000	-	10 min	TEM, high resolution TEM, SEM, Raman spectroscopy, FTIR, energy-dispersive X-ray analysis, powder XRD, Boehm's titration, and N2 adsorption–desorption technique	4 months
8	Lee et al. (2013) [56]	DI water	Power sonic 420	-	3 h	SEM, TEM	-
9	Ghozatloo et al. (2014) [57]	DI water	Ultrasonication	-	15 min	SEM and Raman spectroscopy	-
10	Kim et al. (2014) [58]	DI water	Ultrasonication	400 W, 20 kHz	1 h	TEM, SAED	-

Table 4. *Cont.*

S. No.	Author	Base Fluid	Dispersion Technique	Power	Time	Characterization	Stability Duration
11	Zhang et al. (2014) [60]	Carbon ionic liquid	Ultrasonication	-	24 h	Raman spectroscopy, XPS, and high-resolution TEM	-
12	Ahn et al. (2014) [61]	DI water	High intensity ultrasonic processor	750 W	30 min	SEM	-
13	Liu et al. (2014) [62]	Ionic liquid 1-hexyl-3-methylimidazolium tetrafluoroborate	Sonication followed by ultrasonic cracking	100 W, 40 kHz followed by 25 W	8 h	-	-
14	Sadaghinezhad et al. (2014) [64]	DI water	High power ultrasonication	750 W, 20 kHz	-	-	-
15	Liuet et al. (2015) [66]	Ionic liquid 1-hexyl-3-methylimidazolium tetrafluoroborate	Ultrasonication	-	30 min	Spectrophotometer	-
16	Sadaghinezhad et al. (2015) [67]	DI water	High power ultrasonicator	750 W, 20 kHz	-	UV-VIS, SEM, TEM	30 days
17	Yudong et al. (2015) [68]	DI water	Ultrasonication	300 W, 20 kHz	150 min	STEM	6 months
18	Mehrali et al. (2015) [70]	DI water	Ultra-power high sonicator	1200 W, 20 kHz	-	-	-
19	Mehrali et al. (2015) [71]	DI water	Ultrasonication	1200 W, 20 kHz	-	dispersion analyzer centrifuge.	-
20	Ijam et al. (2015) [72]	DI water + EG(60:40)	Ultrasonication	280 W, 40 kHz	2 h	UV-VIS Spectrometer	-
21	Liu et al. (2015) [73]	DI water	Ultrasonication	20 kHz	150 min	AFM	6 months
22	Kamatchi et al. (2015) [74]	DI water	Ultrasonication	-	12h	XRD, Raman Spectra, FTIR, SEM, AFM	10 days
23	Fan et al. (2015) [75]	DI water	Ultrasonication	-	10 min	DLS, SEM, AFM, TEM	-
24	Esfahani et al. (2016) [77]	DI water	Ultrasonication	130W, 42KHz	1 h	XRD, SEM, UV–Vis spectrophotometry	-
25	Kim et al. (2016) [78]	DI water	Ultrasonication	-	6 h	SEM	-
26	Iranmanesh et al. (2016) [79]	DI water	Ultrasonication	1200 W, 20 kHz	-	-	600 h
27	Tahani et al. (2016) [81]	DI water	Ultrasonication	700 W, 20 kHz	45 min	SEM, XRD	-
28	Vakili et al. (2016) [82]	DI water	Ultrasonication	700 W, 20 kHz	1 h	TEM, XRD	-
29	Vakili et al. (2016) [85]	DI water	Ultrasonication	600 W, 20 kHz	1 h	TEM, XRD, UV-VIS	45 days
30	Tharayil et al.(2016) [87]	DI water	Ultrasonication	-	30 min	PARTICLE SIZE ANALYSER	Less than 3 months
31	Khosrojerdi et al. (2016) [88]	DI water	Ultrasonication	700 W, 20 kHz	1 h	TEM, XRD	-
32	Vakili et al. (2017) [92]	DI water	Ultrasonication	700 W, 20 kHz	1 h	TEM, XRD	-
33	Ranjbarzadeh et al. (2017) [93]	DI water	Ultrasonication	400 W, 28 kHz	4.5 h	SEM, XRD	3 months
34	Tharayil et al. (2017) [94]	DI water	Ultrasonication	-	30 min	TEM	-
35	Khosrojerdi et al. (2017) [95]	DI water	Ultrasonication	700 W, 20 kHz	45 min	SEM, XRD	60 days
36	Zang et al. (2017) [96]	DI water	Ultrasonication	-	1 h	TEM, FTIR, DLS	15 days

Table 4. *Cont.*

S. No.	Author	Base Fluid	Dispersion Technique	Power	Time	Characterization	Stability Duration
37	Liu et al. (2017) [97]	DI water	Ultrasonication	300 W	150 min	Laser Size Analyzer	60 days
38	Chen et al. (2017) [98]	DI water	Ultrasonication	-	5 min	Particle Size Analyser, Uv-Vis Nir Spectrometer	-
39	Iranmanesh et al. (2017) [99]	DI water	Ultrasonication	-	-	TEM, SEM	3 months
40	Wang et al. (2017) [100]	WD type synthetic oil	Ultrasonication	-	-	Microscopic Imaging System	30 days
41	Chai at al. (2017) [101]	Hydrogenated oil	Ultrasonication	320 W, 40 kHz	3 h	-	-

2.3.2. Covalent Method

Covalent technique involves the treatment of graphene nanoplatelets with concentrated acid without the use of any surfactant. This acid treatment attaches the hydrophilic functional groups, such as acid group, hydroxyl ions, on the plane surface of the graphene layers, as shown in the Figures 3 and 4, which increases the stability and dispersion of the graphene nanoplatelets in the base fluid.

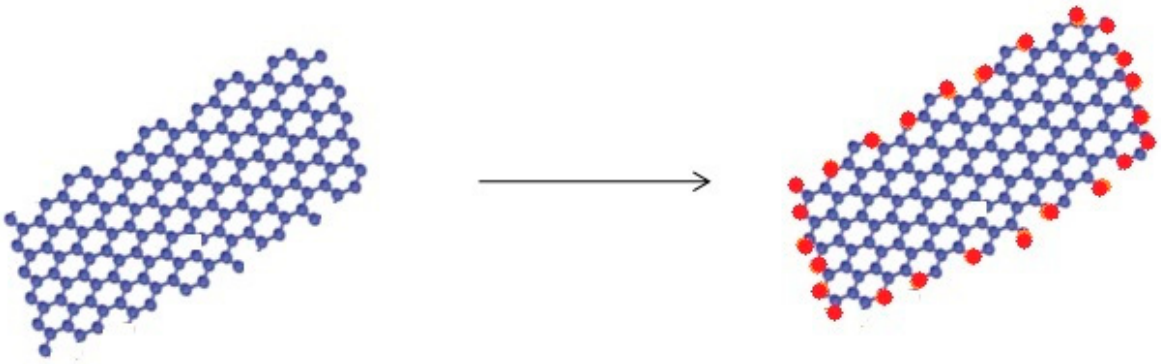

Figure 3. Acid-treated graphene nanoplatelets.

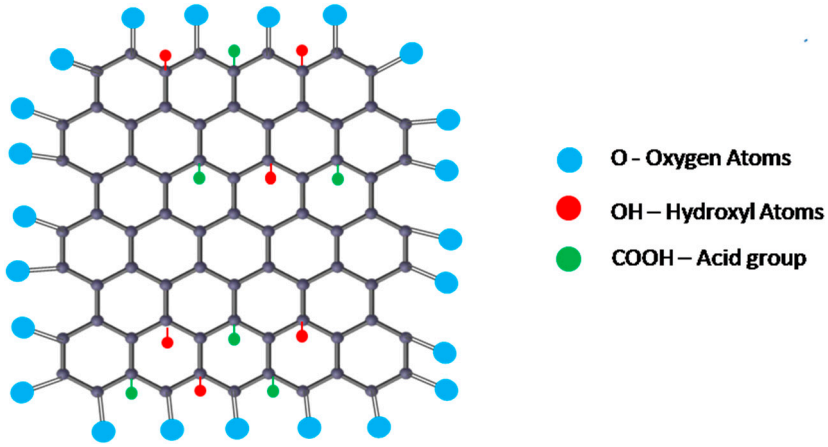

Figure 4. Structure of functionalized graphene.

Gupta et al. (2011) [29] prepared graphene-dispersed water nanofluids using covalent technique treating with sulfanilic acid. They used sulfonation as a dispersion technique for two hours and found the prepared nanofluids stable for more than six months. Baby et al. (2011) [30] prepared a stable DI water and Ethylene Glycol based graphene nanofluids

by treating the particles with sulphuric acid and nitric acid in the ratio of 3:1 using an ultrasonic water bath.

Ghozatloo et al. (2013) [31] prepared graphene nanoplatelets/water-based nanofluids ranging from 0.005–0.023 vol% using the two-step method. The functionalization process was carried out by treating it with potassium per sulfate and it provides a good stability and dispersion of graphene for about seven days. Maa et al. (2013) [32] used silicone oil as a base fluid for the dispersal of the functionalized graphene nanoplatelets with the composition varying from 0.004, 0.013, 0.022, and 0.031 vol% using the two-step method. The observation indicated the presence of a small quantity of visual sedimentation after ten days. Kole et al. (2013) [33] prepared EG/Water-based (30/70) graphene nanofluids using acid treatment with sulphuric acid and nitric acid in the ratio of 3:1 and ultrasonic dispersion technique for more than two hours. The prepared nanofluids were stable for more than 150 days. Ghozatloo et al. (2013) [34] prepared a stable graphene dispersed ethylene glycol nanofluids through the use of the covalent method and the sonication technique for about 45 min.

Farid et al. (2015) [35] used nitrogen-doped activated carbon graphene in ethylene glycol and no sedimentation and agglomeration was found over a period of several hours for all concentrations, 0.01, 0.02, and 0.03 vol% due to the use of functionalization technique involved. Amiri et al. (2015) [36] prepared GnP/ H_2O nanofluids of 0.011, 0.023, and 0.045 vol% using both covalent and noncovalent (SDBS) functionalization. Dispersion results illustrated no sedimentation after one month under ambient conditions. Amiri et al. (2015) [37] repeated the experiments by treating with hydrochloric acid and ethylene glycol as a base fluid and the prepared nanofluids were found to be stable for more than a month. Arzani et al. (2015) [38] again confirmed the stability characteristics of graphene-dispersed water nanofluids using the same ratio of sulphuric acid and nitric acid as used by the previous researchers.

Sarsam et al. (2016) [39] prepared a triethanolamine-treated graphene/water nanofluids of different concentrations, namely, 0.011, 0.023, 0.034, and 0.045 vol%. This method of covalent functionalization resulted in reaching a higher stability for 0.045 vol% showing 12.4% sedimentation after 100 days. Moarzani et al. (2016) [40] prepared stable graphene-distilled water nanofluids treating them with red wine in a nitrogen environment and found that the nanofluids were stable for several days. Yarmand et al. (2016) [41] prepared distilled water-based graphene nanofluids with acid treatment of sulphuric acid and nitric acid in the ratio 3:1 and the prepared nanofluids were found stable for 240 h. Agromayor et al. (2016) [42] dispersed sulfonic-acid-treated graphene in water using 200 W, 20 kHz sonicator for about 240 min and the prepared nanofluids were found to be stable. Solangi et al. (2016) [43] prepared graphene dispersed propylene glycol treated water nanofluids using acid treatment of sulphuric acid and nitric acid in the ratio 3:1 and the prepared fluids were found to be stable for more than 30 days.

Sadri et al. (2017) [44] conducted experiments by preparing covalent functionalized graphene/DI water nanofluids of 0.05 vol% treated with gallic acid and the zeta potential values of −30.6 to −50.7mv showed a good dispersion stability even after 34 days. Amiri et al. (2017) [45] used covalent functionalization method for the preparation of 0.000455 and 0.00091 vol% of graphene/water nanofluids and reported the higher concentration having higher zeta potential value of 49.2 to 52 mv. A decrease in value was seen with decreasing vol%. Amiri et al. (2017) [46] used covalent functionalization of graphene nanoparticles treated with amine dispersed in a transformer oil to prepare 0.0041 vol% of nanofluids and reported the degradation rate of the sample as less than 0.5% after a month, indicating effective colloidal stability of the suspension under visible light irradiation. Esfahani et al. (2017) [47] used the two-step method and 130 W, 42 kHz sonicator for the preparation of 0.00455 and 0.045 vol% of GnP/H_2O nanofluids treated with concentrated sulphuric acid and zeta potential values of −32 & −41 mv, confirming its good stability.

Sidney et al. (2019) [109] prepared distilled water based functionalized graphene nanofluids with concentrations varying from 0.1 vol% to 0.5 vol% and reported the fluid

as remaining stable for a long period of time due to acid treatment of nanoplatelets. Vishnuprasad et al. (2019) [110] prepared deionized water based functionalized graphene nanofluids using nitric acid/sulphuric acid with concentrations varying from 0 vol% to 0.2 vol% and reported the fluid remaining stable for a long duration of time due to functionalization. Saeed et al. (2019) [111] used the two-step method and 80 W, 50–60 Hz sonicator for the preparation of GnP/Propylene glycol nanofluids treated with concentrated sulphuric acid, confirming its good stability. Balaji et al. (2020) [113] prepared distilled water-based functionalized graphene nanofluids with concentration varying from 0.01 vol% to 0.2 vol% and reported the fluid remaining stable for one month due to the acid treatment of the nanoplatelets. Table 5 provides a summary of the published literature on synthesis of graphene nanofluids by covalent method.

Table 5. Summary of published literature on synthesis of graphene nanofluids by the covalent method.

S. No.	Author/Year	Base Fluid	Acid	Dispersion Technique	Power	Time	Characterization	Stability Duration
1	Gupta et al. (2011) [29]	DI water	Sulfanilic acid	Sulfonation	-	2 h	TEM, DLS, UV Vis absorption	6 months
2	Baby et al. (2011) [30]	DI water, EG	Sulphuric acid/nitric acid (3:1)	Ultrasonication	-	30–45 min	Powder XRD, electron microscopy, Raman and FTIR spectroscopy	-
3	Ghozatloo et al. (2013) [31]	DI water	Potassium persulfate	Ultrasonication	-	1 h	SEM, TEM, Raman spectroscopy, FTIR spectroscopy	7 days
4	Maa et al. (2013) [32]	Silicone oil	3-glycidox-ypropyltrimetho-xysilane	Ultrasonication	-	6 h	FTIR spectroscopy, AFM Raman spectroscopy, UV–vis spectroscopy, XRD	10 days
5	Kole et al. (2013) [33]	EG/Water(30/70)	Sulphuric acid/nitric acid (3:1)	Ultrasonication	-	2 h	XRD, TEM, Raman spectroscopy, and FTIR spectroscopy	150 days
6	Ghozatloo et al. (2013) [34]	Ethylene glycol	Sulphuric acid/nitric acid (3:1)	Ultrasonication	-	45 min	XRD, SEM, TEM	-
7	Farid et al. (2015) [35]	Ethylene glycol	Sulphuric acid/nitric acid (3:1)	Ultrasonication	-	40 min	SEM, TEM, Raman Microscope, XPS	Several hours
8	Amiri et al. (2015) [36]	DI water	Sulphuric acid/nitric acid (3:1)	Ultrasonication	-	10 min	FTIR, TEM	1 month
9	Amiri et al. (2015) [37]	Eg/water (40/60)	Hydrochloric acid	Ultrasonication	-	10 min	vibration spectroscopie, temperature-programmed study, microscopic method	1 month
10	Arzani et al. (2015) [38]	DI water	Sulphuric acid/nitric acid (3:1)	Ultrasonication	-	-	-	-
11	Sarsam et al. (2016) [39]	DI water	Triethanolamine	Ultrasonication	-	-	FTIR, Raman spectroscopy, EDS, and TEM	100 days
12	Mehrali et al. (2016) [40]	DI water	Red wine treated in nitrogen atmosphere	Ultrasonication	-	-	XRD, XPS, FTIR, UV visible spectrometer, SEM, TEM	-

Table 5. *Cont.*

S. No.	Author/Year	Base Fluid	Acid	Dispersion Technique	Power	Time	Characterization	Stability Duration
13	Yarmand et al. (2016) [41]	DI water	Sulphuric acid/nitric acid (3:1)	Ultrasonication	-	-	XRD, SEM, FTIR and Raman	240 h
14	Agromayor et al. (2016) [42]	DI water	Sulfonic acid	Ultrasonication	200 W, 20 kHz	240 min	SEM, EDS	-
15	Solangi et al. (2016) [43]	Propylene glycol treated water	Sulphuric acid/nitric acid (3:1)	Ultrasonication	-	-	FTIR, Raman spectrum, SEM, TEM	34 days
16	Sadri et al. (2017) [44]	DI water	Gallic acid	Ultrasonication	=	15 min	XPS, TEM	34 days
17	Amiri et al. (2017) [45]	DI water	Sulphuric acid/nitric acid (3:1)	Ultrasonication	20 kHz, 750 W	-	XPS, AFM, UV–vis spectrometry	1 month
18	Amiri et al. (2017) [46]	Transformer oil	Sulphuric acid/nitric acid (3:1)	Ultrasonication	300 W	30 min	AFM, UV-VIS	1 month
19	Esfahani et al. (2017) [47]	DI Water	Conc sulphuric acid	Ultrasonication	130 W, 42 kHz	1 h	XRD, SEM, DLS	-
20	Sidney et al. (2019) [109]	DI Water	Con. Nitric acid	Ultrasonication	700 W, 20 kHz	2 h	SEM, TEM	-
21	Vishnuprasad et al. (2019) [110]	DI water	Nitric acid/sulphuric acid	Ultrasonication	20 kHz	-	SEM, Raman spectrum	-
22	Saeed et al. (2019) [111]	Propylene glycol	Sulphuric acid	Ultrasonication	50–60 Hz, 80 W	-	SEM, XPS, FTIR	-
23	Balaji et al. (2020) [113]	DI Water	Con. Nitric acid	Ultrasonication	700 W, 20 kHz	2h	SEM	1 month

Many researchers have carried out the preparation of GnP base nano dispersion under the covalent technique, which involved the attachment of acidic functional group on the basal planes of GnP. Stability of the prepared dispersion remains for a longer period of time without any settlement has been reported. This is the major requirement for any nanofluids in practical applications. It was also observed that, the GnP was treated with different acid combinations and shows the similar and better stability for a same period of time after preparation, irrespective of the acid treatment.

2.3.3. Non-Covalent Method

The non-covalent technique involves the use of a surfactant for the dispersal of GnP in the base fluid which increases the stability of the prepared nanofluids. The process involved in the preparation of GnP nanofluids using the non-covalent technique is shown in Figure 5.

Yu et al. (2011) [49] used sodium dodecyl benzene sulphonate (SDBS) as a surfactant for the dispersal of graphene in distilled water. The prepared nanofluids were found stable for several days without any settlement. Jiaa et al. (2014) [59] prepared water-based graphene nanofluids of 0.045 vol% using sodium dodecyl sulfonate (SDS) and carboxyl methyl cellulose (CMC) as a surfactant. The stability results indicated the CMC added nanofluid having a lower zeta potential value as compared with SDS indicating a good dispersion. Li et al. (2014) [63] prepared graphene/H_2O nanofluids in concentrations of 0.00455, 0.00682, 0.0091, and 0.045 vol%. Sodium dodecyl benzene sulphonate was added as a surfactant to improve stability. Sedimentation was not observed less than 6 h after the addition of the surfactant. Zanjani et al. (2014) [65] used poly vinyl alcohol (PVA) as a surfactant for the preparation of stable graphene-dispersed distilled water nanofluids.

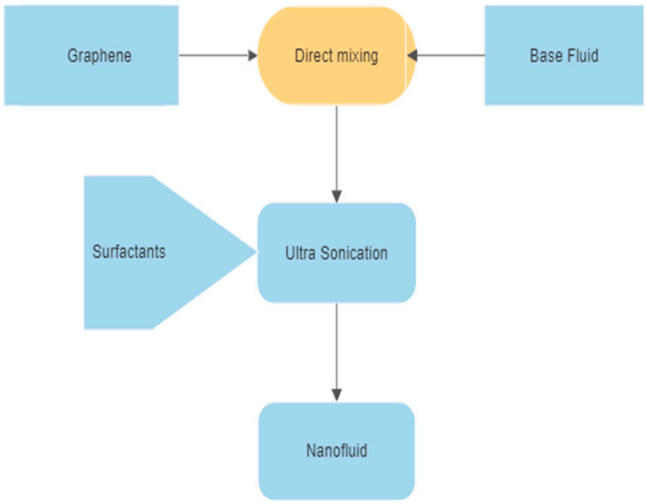

Figure 5. Non-covalent technique.

Leia et al. (2015) [69] used paraffin-based GnP nanofluids of 0.02 vol%. Sodium dodecyl benzene sulphonate was used as a surfactant for stability. Graphene nanoplatelets dispersed better with the action of electromagnetic field during solidification. Askari et al. (2016) [76] prepared 0.045 vol% of graphene-dispersed water nanofluids using the two-step method. Zeta potential value is found to be −43.5 mV indicating a stability for a long time. Naghash et al. (2016) [80] added Ter-polymer as a surfactant for the preparation of stable graphene/DI water nanofluids of different concentrations, 0.014, 0.022, and 0.045 vol%. Zanjani et al. (2016) [83] conducted experiments on graphene/DI water nanofluids of different concentrations 0.005, 0.01, and 0.02 vol% prepared by the two-step method. However, the authors have not reported the stability conditions of the nanofluids.

Jiaa et al. (2016) [84] used sodium carboxy methyl cellulose as a surfactant for the preparation of stable DI water-based graphene nanofluids of 0.0022 vol% and reported the nanofluids remained stable for one month having zeta potential value of 53.1 mv. Sarsam et al. (2016) [86] used a non-covalent functionalization method using different surfactants such as (CTAB) cetyl trimethyl ammonium bromide, (GA) gum Arabic, (SDBS) sodium dodecyl benzene sulfonate, (SDS) sodium dodecyl sulfate, for the preparation of stable graphene-dispersed DI water nanofluids of 0.045 vol% and the stability tests was reported that the zeta potential value of 45.6 mV is higher for SDBS nanofluid showing greater stability as compared with other nanofluids.

Ahammed et al. (2016) [89] used sodium dodecyl benzene sulfonate as a surfactant for the preparation of stable nanofluids. Agarwal et al. (2016) [90] used three different surfactants, Oleic acid, oleylamine, and tween20 to disperse graphene in kerosene and found the nanofluids stable for 20–30 days. Goodarzi et al. (2016) [91] used Triton100 non-ionic surfactant for the preparation of stable graphene nanofluids. Sonication was done using 1200 W, 20 kHz sonicator. The prepared nanofluids were found to be stable for more than 200 days. Ali et al. (2017) [102] used polyvinyl pyrrolidone as a surfactant to prepare distilled water-based graphene nanofluids in a ultrasonicator of about 200 W, 25 kHz for 4 h and found the nanofluids stable for more than 2 months. Arshad et al. (2017) [103] used the same technique and surfactant as used by Ali et al. [102] and found that the nanofluids remain stable for more than 2 months.

Selvam et al. (2017) [104–108] used sodium deoxycholate (SDC) as a surfactant for the preparation of graphene dispersed in three different base fluids, namely, distilled water, ethylene glycol, and EG/water mixture [30/70] and found the nanofluids to be stable for 3 months. Das et al. (2019) [112] used Gum acacia as a surfactant for the preparation of graphene dispersed in DI water and found the nanofluids stable for 30 days.

A summary of published literature on synthesis of graphene nanofluids by non-covalent method using chemical technique has been provided in Table 6. Many researchers

have prepared GnP-based nanofluids using a non-covalent technique. This technique involved the addition of surfactant into the base fluid for better stability. Several surfactants were used for the preparation of GnP nanofluids. All the surfactant increased the stability for certain period without any sedimentation. The major disadvantage of using the surfactant in the increment in the density and viscosity of the GnP nanofluids which, in turn, increased the pumping power and the pressure drop effectively. The addition of surfactant also enhances the thermal boundary resistance of GnP with the surrounding molecules limiting the thermal transport properties. Hence this method can be used in the areas where the stability is the major requirement without consideration of thermal properties, pumping power, and the pressure drop, respectively.

Table 6. Summary of published literature on synthesis of graphene nanofluids by non-covalent method.

S. No.	Author	Base Fluid	Surfactant	Molecular Formula	Dispersion Technique	Power	Time	Characterization	Stability Duration
1	Yu et al. (2011) [49]	Ethylene glycol	Sodium dodecyl benzene sulfonate (SDBS).	$C_{18}H_{29}NaO_3S$	Ultrasonication	-	5 min	TEM, AFM	-
2	Jiaa et al. (2014) [59]	DI water	Sodium dodecyl sulfonate (SDS) and carboxyl methyl cellulose (CMC)	$C_{18}H_{29}NaO_3S$	Ultrasonication	-	2 h	-	1 week
3	Li et al. (2014) [63]	DI water	Sodium dodecyl benzene sulphonate	$C_{18}H_{29}NaO_3S$	Ultrasonication	-	1 h	TEM	6h
4	Zanjani et al. (2014) [65]	DI water	Poly Vinyl Alcohol	$(C_2H_4O)x$	Ultrasonication	-	-	AFM, UV-VIS	-
5	Leia et al. (2015) [69]	parrafin	Sodium dodecyl benzene sulphonate	$C_{18}H_{29}NaO_3S$	Ultrasonication	-	1 h	SEM	-
6	Askari et al. (2016) [76]	DI water	Gum arabic, Tween80, ctab, triton x100, and acumer terpolymer	$C_{64}H_{124}O_{26}$ $C_{19}H_{42}BrN$ $C_{14}H_{22}O(C_2H_4O)_n$ (n = 9–10)	Ultrasonication	130 W	15 min	SEM, TEM	Two months
7	Naghash et al. (2016) [80]	DI water	Ter-polymer	-	Ultrasonication	-	-	TEM, BET and XRD	-
8	Zanjani et al. (2016) [83]	DI water	Poly Vinyl Alcohol	$(C_2H_4O)x$	Ultrasonication	-	-	AFM	-
9	Jiaa et al. (2016) [84]	DI water	Sodium carboxymethyl cellulose	$C_8H_{15}NaO_8$	Ultrasonication	600 W, 40 kHz	2 h	SEM, EDS, UV-VIS	1 month
10	Sarsam et al. (2016) [86]	DI water	(CTAB)cetyl trimethyl ammonium bromide, (GA) gum Arabic, (SDBS) sodium dodecyl benzene sulfonate, (SDS) sodium dodecyl sulfate	$C_{19}H_{42}BrN$ $NaC_{12}H_{25}SO_4$ $C_{18}H_{29}NaO_3S$	Ultrasonication	750 W, 20 kHz	120 min	TEM, UV-VIS	60 days
11	Ahammed et al. (2016) [89]	DI water	Sodium dodecyl benzene sulphonate (SDBS)	$C_{18}H_{29}NaO_3S$	Ultrasonication	-	30 min	SEM	-
12	Agarwalet al. (2016) [90]	Kerosene	Oleic acid, oleylamine, tween- 20	$C_{18}H_{34}O_2$ $C_{18}H_{35}NH_2$ $C_{58}H_{114}O_{26}$	Ultrasonication	-	40 min–3 h	DLS	20–30 days
13	Goodarzi et al. (2016) [91]	DI water	Triton x 100 non-ionic surfactant	$C_{14}H_{22}O(C_2H_4O)_n$ (n = 9–10)	Ultrasonication	1200 W, 20 kHz	60 min	SEM, TEM, XPS,	200 days
14	Ali et al. (2017) [102]	DI water	Polyvinyl pyrrolidone (PVP)	$(C_6H_9NO)_n$	Ultrasonication	200 W, 20–25 kHz	1/2 h to 4 h	-	2 months

Table 6. *Cont.*

S. No.	Author	Base Fluid	Surfactant	Molecular Formula	Dispersion Technique	Power	Time	Characterization	Stability Duration
15	Arshad et al. (2017) [103]	DI water	Polyvinyl pyrrolidone (PVP)	$(C_6H_9NO)_n$	Ultrasonication	200 W, 20–25 kHz	1/2 h to 4 h	-	2 months
16	Selvam et al. (2016) [104]	Ethylene glycol and water	Sodium deoxy cholate	$C_{24}H_{39}NaO_4$	Ultrasonication	700 W, 20 kHz	2 h	SEM, UV-VIS	15 days
17	Selvam et al. (2017) [105]	EG/Water (30/70)	Sodium deoxy cholate	$C_{24}H_{39}NaO_4$	Ultrasonication	700 W, 20 kHz	2 h	SEM	3 months
18	Selvam et al. (2017) [106]	EG/Water (30/70)	Sodium deoxy cholate	$C_{24}H_{39}NaO_4$	Ultrasonication	700 W, 20 kHz	2 h	SEM, TEM	15 days
19	Selvam et al. (2017) [107]	EG/Water (30/70)	Sodium deoxy cholate	$C_{24}H_{39}NaO_4$	Ultrasonication	700 W, 20 kHz	2 h	SEM, TEM, UV-VIS	15 days
20	Selvam et al. (2017) [108]	EG/Water (30/70)	Sodium deoxy cholate	$C_{24}H_{39}NaO_4$	Ultrasonication	700 W, 20 kHz	2 h	SEM, TEM, UV-VIS	15 days
21	Das et al. (2019) [112]	DI Water	Gum acacia	$C_{15}H_{20}NNaO_4$	Ultrasonication	-	5 h	SEM	30 days

3. Thermophysical Properties

3.1. Thermal Conductivity of Nanofluids with Graphene

Heat transfer phenomenon of any nanofluids is mainly characterized by thermos-physical properties such as thermal conductivity, density, viscosity, specific heat, surface tension, etc. Among the thermos-physical properties, thermal conductivity is the major driving property for nanofluids. Graphene-based nanofluids possess a high potential in the heat transfer application areas due to its high intrinsic thermal conductivity. Several researchers measured the thermal conductivity of graphene-based nanofluids for the past few years which we summarize in this article.

3.1.1. Thermal Conductivity Measurement

Various techniques were available for the measurement of the thermal conductivity of nanofluids, such as:

- Transient hot wire method;
- Temperature oscillation method;
- 3-ω method.

There are specific non-intrusive optical measurement techniques: forced Rayleigh scattering and infrared microscopy for thermal conductivity measurements. These techniques are costly even though the elimination eliminates the uncertainty issues associated with steady-state and transient hot wire methods due to the diffusion and aggregation of nanomaterials and the occurrence of natural convection during long measurement times. The specific error sources are temperature variation and non-linear heat flow. Temperature variation at contact surfaces can occur in two forms, a progressive drift in the overall temperature and a temporary fluctuation across the platen surface. The analysis shows that the uncertainty of the thermal conductivity measurement is about ±3.3% for 68% confidence level. Hence the transient hot wire technique is the most adopted method for the measurement of the thermal conductivity of nanofluids. The experimental setup consists of a platinum (Pt) hot wire of certain length with an electrically insulating coating to avoid the errors associated with the electrical conduction of nanoparticles. The hot wire is soldered to electrically insulated lead wires to keep the wire straight and also to connect it to the electrical system. The test cell is made of metal/Al/brass which is immersed in a thermostatic bath to precisely control the temperature of the fluids in which the experiments were performed.

The soldered hot wire was connected to a Wheatstone bridge which has two high precision fixed resistors and one variable resistor. Two arms of the bridge were considered as the fixed resistors with the rest two arms assigned for the variable resistor and transient

hot wire. A constant voltage supply was supplied to the system for a period of few seconds. The electrical impulse will disrupt the bridge balance and cause a change in resistance of the hot wire due to the change in temperature. Change in resistance of the wire during this period was acquired using a data logger at a sampling interval.

3.1.2. Thermal Conductivity of Aqueous Based Graphene Nanofluids

Much research has been conducted for the measurement of the thermal conductivity of aqueous graphene dispersed nanofluids. Gupta et al. (2011) [29] measured the thermal conductivity of GnP/H_2O by the use of the transient hot wire method and found that the enhancement in thermal conductivity is mainly due to Brownian motion, micro convection effects. The maximum enhancement in thermal conductivity was found to be 27% at 0.2 vol% in their research. Baby et al. (2011) [30] measured the thermal conductivity of water-based graphene nanofluids using transient hot wire method and found the maximum enhancement as 75% at 0.05 vol%. Ghozatloo et al. (2013) [31] observed an enhancement of about 18% at 0.023 vol% of graphene in distilled water.

Amiri et al. (2015) [36] worked on GnP/H_2O based nanofluids and reported the enhancement of thermal conductivity of about 28.125% at 0.045 vol% at 50 °C respectively due to Brownian motion and formation of surface nanolayer. Arzani et al. (2015) [38] observed enhancement of 10.58% at 0.045 vol% of graphene suspended in distilled water.

Sarsam et al. (2016) [39] determined the enhancement of thermal conductivity of about 25% at 0.045 vol% at 40 °C in a triethanolamine-treated GnP/H_2O based nanosuspension using the Transient hot wire method and reported the aspect ratio, differential effective medium (DEM) as the major reasons for the enhancement. Mehrali et al. (2016) [40] observed an enhancement of about 47.54% at 4 vol% of graphene suspended in distilled water. Yarmand et al. (2016) [41] measured the thermal conductivity using the transient hot wire method for graphene dispersed water nanofluids and found enhancement in the thermal conductivity by 15.87% at 0.045 vol%. Agromayor et al. (2016) [42] observed enhancement of about 12.69% at 1 vol% of graphene suspended in water. Sadri et al. (2017) [44] conducted experiments on graphene dispersed in distilled water and measured the thermal conductivity using the transient hot wire method. The results showed the thermal conductivity enhanced by 24.18% at 0.05 vol% of graphene. Amiri et al. (2017) [45] observed the thermal conductivity enhancement of about 22.58% at only 0.00091 vol% of graphene dispersed in water. Esfahani et al. (2017) [47] measured the thermal conductivity for graphene dispersed water nanofluids and found the enhancement as 18.9% at 0.045 vol% respectively.

Jyothirmayee et al. (2011) [48] worked on GnP/H_2O, EG based nanofluids and reported the enhancement of thermal conductivity as about 6.5% and 13.6% at 25 °C for 0.14 vol% for water and EG respectively due to shape effect and size effect of the nanoplatelets.

Ghozatloo et al. (2014) [57] prepared GnP/H_2O based nanofluids and reported the thermal conductivity enhancement as about 31.83% at 0.075 vol% of graphene loading measured by transient hot wire method. Sadaghinezhad et al. (2014) [64] observed an enhancement of about 23.80% at 0.045 vol% of graphene suspended in distilled water. Zanjani et al. (2014) [65] observed the enhancement of about 10.3% at 0.02% for graphene dispersed water nanofluids.

Mehrali et al. (2015) [70,71] observed the enhancement in thermal conductivity of about 29.03% at 0.045 vol% of graphene dispersed in distilled water. Kamatchi et al. (2015) [74] reported the Brownian motion of the nanoplatelets as the major reason for thermal conductivity enhancement of about 10% at 0.3g/L in RGO/H_2O based nanofluids.

Askari et al. (2016) [76] observed the enhancement in thermal conductivity of about 16% while dispersing 0.045 vol% of graphene in distilled water. Esfahani et al. (2016) [77] measured the thermal conductivity for graphene dispersed water nanofluids and found a 56% enhancement in the thermal conductivity at 0.227 vol% of nanoplatelets. Iranmanesh et al. (2016) [79] Prepared a GnP/ H_2O based nanofluids and reported thermal conductivity

enhancement of about 8.14% at 0.045 vol% of graphene loading at 60 °C measured using the transient hot wire method. Flagging of the intermolecular adhesion forces was found as the possible mechanism for enhancement in his work. Amiesahel et al. (2016) [80] observed the minimum enhancement of about 1.18% as made comparison with the base fluid at 0.045 vol% of graphene suspended in water. Tahani et al. (2016) [81] observed 11.47% enhancement in thermal conductivity of graphene water nanofluids at 0.045 vol% of nanoplatelets.

Zanjani et al. (2016) [83] observed enhancement of about 9.52% at 0.02 vol% of graphene nanoplatelets suspended in distilled water. Vakili et al. (2016) [85] measured the thermal conductivity of graphene deionized water nanofluids and reported a 15% enhancement in the thermal conductivity at 0.0022 vol% of nanoplatelets. Sarsam et al. (2016) [86] observed a 11.48% enhancement in thermal conductivity at 0.045 vol% of graphene dispersed in distilled water. Tharayil et al. (2016) [87] observed enhancement of about 27.6% at 0.009 vol% of graphene dispersed in distilled water. Khosrojerdi et al. (2016) [88] used transient short hot wire technique for determination of thermal conductivity of GnP/H_2O based nanofluids. Enhancement of the thermal conductivity was found to be 14.75% at 0.0022 vol%. Ahammed et al. (2016) [89] conducted experiments on GnP/H_2O based suspensions and measured the thermal conductivity using the transient short hot wire technique. The phonons, free electrons and molecular collision and diffusion were seen as the feasible mechanisms for the enhancement of thermal conductivity by 37.12% at 0.15 vol% at 50 °C in the experiments. Goodarzi et al. (2016) [91] observed a 10.025% enhancement in thermal conductivity at 0.06 vol% of graphene water nanofluids.

Ranjbarzadeh et al. (2017) [93] measured the thermal conductivity of graphene water nanofluids at room temperature. Enhancement was found to be 31% respectively. Khosrojerdi et al. (2017) [95] used the transient short hot wire technique for determination of thermal conductivity of GnP/H_2O based nanofluids and the enhancement of the thermal conductivity was found to be 13% at 0.045 vol% at 50 °C due to the brownian motion of the nanoplatelets. Chen et al. (2017) [98] measured the thermal conductivity of graphene water nanofluids. Enhancement was found to be 42.3% at 0.1 vol% of graphene. Iranmanesh et al. [99] conducted the experiments on water graphene nanofluids and reported that the enhancement in thermal conductivity was found to be 36.36% at 0.045 vol%.

Selvam et al. (2016) [104] conducted experiments on GnP/EG and H_2O based nanofluids using the transient hot wire technique and concluded that several mechanisms such as high aspect ratio, geometry were involved in the enhancement of thermal conductivity of about 21% for EG based nanofluids while it was 16% for water. Shaji et al. (2019) [109] measured the thermal conductivity of functionalized graphene nanofluids using the transient hot wire technique and reported the maximum enhancement in thermal conductivity as 23.78% due to GnP size and two dimensional geometry of GnP respectively. Vishnuprasad et al. (2019) [110] measured the thermal conductivity of functionalized graphene nanofluids using the transient hot wire technique and reported the maximum enhancement in thermal conductivity as 55.38% due to high thermal conductivity of GnP and Brownian motion of the nanoparticles respectively. Das et al. (2019) [112] measured the thermal conductivity of graphene water nanofluids at 25 °C and the enhancement was found to be 17%. However, enhnacement was found to be 29% at 45 °C for higher concentration of graphene nanofluids. The free conduction electrons at high energy levels and Brownian motion were found to be cause of the thermal conductivity enhancement. Balaji et al. (2020) [113] measured the thermal conductivity of functionalized graphene nanofluids using the transient hot wire technique and reported the maximum enhancement in thermal conductivity as 11% at 0.2 vol% due to GnP size and two dimensional geometry of GnP respectively.

3.1.3. Thermal Conductivity of Non-Aqueous Based Graphene Nanofluids

Several researches were also conducted on various non aqueous based graphene dispersions for wide areas of application and measured the thermal conductivity of non aqueous dispersion as follows. Maa et al. (2013) [32] suspended the graphene nanoplatelets

in silicone oil and measured the thermal conductivity enhancement using the transient hot wire method. The thermal conductivity value enhances by 18.5% at 0.07 vol% of GnP.

Kole et al. (2013) [33] determined the enhancement of thermal conductivity as 15% at 0.395 vol% of GnP /EG-H_2O (70:30) base fluid at room temperature by the transient hot wire method. It was reported that the matrix-additive interface contact resistance of mis-oriented ellipsoidal particles is the major reason for the enhancement. Ghozatloo et al. (2013) [34] observed the thermal conductivity enhancement of about 21.2% at 0.15 vol% of graphene suspended in ethylene glycol at room temperature. Farid et al. (2016) [35] suspended the graphene nanoplatelets in ethylene glycol and measured the thermal conductivity using the transient hot wire method. It was observed that the thermal conductivity enhances by 10.16% for 0.03 vol% of nanoplatelets at higher temperature.

Amiri et al. (2015) [37] measured the thermal conductivity of GnP—(EG + H_2O) by the transient hot wire method and concluded that the enhancement in thermal conductivity is mainly due to the Brownian motion of nanoplatelets in the base fluid. The maximum enhancement in thermal conductivity was found to be 54.28% at 0.0955 vol% at 65 °C in the research. Solangi et al. (2016) [43] dispersed graphene in a propylene glycol treated water and found that the thermal conductivity enhances by 32.8% at 0.1 vol% as compared with the base fluid. Amiri et al. (2017) [46] repeated the experiments with transformer oil and observed that the increment was found to be 10% at 0.001 vol% of nanoplatelets. Yu et al. (2011) [49] used the transient short hot wire technique to determine the thermal conductivity of GnP/EG based nanofluids. The effect of 2D structure and stiffness of the nanoplatelets enhances the thermal conductivity by 86% at 5% vol% of graphene.

Wanga et al. (2012) [51] conducted experiments on Graphite/ oil based suspensions and measured the thermal conductivity using the transient short hot wire technique. Clustering effect of nanoplatelets enhances the thermal conductivity by 36% at 1.36 vol% in the experiments. Liu et al. (2014) [62] measurement on thermal conductivity of GnP/1-hexyl-3-methylimidazolium tetrafluoroborate ([HMIM] BF4) based suspension using thermal constant analyzer resulted that 0.00374 vol% increases by 15.2% to 22.9% as the tested temperature varies from 25 to 200 °C. Ijam et al. (2015) [72] reported 6.67 to 10.47% enhancement of thermal conductivity at 0.045 vol% for GO −(EG+H_2O)(40/60) based nanofluids using transient hot wire method.

Agarwal et al. (2016) [90] used kerosene as base fluid to disperse graphene and saw thermal conductivity enhancement upto 26.21% at 0.09 vol%. Wang et al. (2017) [100] used synthetic oil as the base fluid for dispersing graphene and 25% enhancement in thermal conductivity was observed at room temperature for 0.2 mg of graphene per mL of base fluid. Chai at al. (2017) [101] worked on GnP/hydrogenated oil based suspensions and reported a 14.41% enhancement in thermal conductivity at 100 ppm of graphene loading using the transient hot wire technique. Selvam et al. (2016) [105–107] reported enhancement of thermal conductivity for GnP/EG-H_2O (30:70) using the transient hot wire technique of about 18% at 0.45 vol% due to two dimensional network and particle clustering. Saeed et al. (2019) [111] used propylene glycol as base fluid for the dispersal of graphene. The thermal conductivity enhanced upto 51.8% at 1.441 vol% in the experiments.

Findings seen in literature show increase in thermal conductivity with respect to the GnP loading and also increase in the temperature. A significant enhancement in thermal conductivity was observed. This was mainly due to the higher thermal conductivity of GnP lying in the range of 1000–3000 W/mK. Several mechanisms were reported for this significant enhancement in thermal conductivity. Predominant researchers have measured the thermal conductivity of GnP nanofluids using the transient hot wire technique. Some have reported the Brownian motion and micro convection effect playing a major role in thermal conductivity enhancement. However, there was a decrease in Brownian diffusion coefficient with increase in viscosity. Hence the inference was that the Brownian motion played a significant role in the thermal conductivity enhancement only in the low viscous fluids and not predominant in high viscous fluids [104]. Some other researchers have reported the enhancement due to the aspect ratio, shape and size of the nanoparticles, two-dimensional

structure and networking of nanoplatelets respectively. Several other mechanisms such as micro convection effects, particle clustering have been reported to be the major cause for the enhancement in thermal conductivity. But still there is no compressive conclusion relating to the exact mechanism responsible for the thermal conductivity enhancement of GnP nanofluids. The conclusion was that the thermal boundary resistance of GnP with the surrounding fluid molecules plays a major role in the thermal conductivity enhancement of the nanofluids. Hence more research on the decrease in the thermal boundary resistance of the graphene with the surrounding base fluids is required. This could effectively enhance the thermal conductivity.

A summary of published literature on thermal conductivity of graphene-based nanofluids has been provided in Table 7.

Table 7. Summary of published literature on thermal conductivity of graphene-based nanofluids.

S. No.	Author/Year	Base Fluid	Measurement Technique	Type	Mechanism	Vol% Range	Temperature Range (°C)	Enhancement (%) at Room Temp	Enhancement (%) at High Temp
1	Gupta et al. (2011) [29]	DI water	Transient hot wire method	Custom built	Brownian motion, micro convection effects	0.05–0.2	30–50	10	28
2	Baby et al. (2011) [30]	DI water, EG	Transient hot wire method	Commercial	-	0.005–0.050.05–0.08	25–50	16 1	75 5
3	Ghozatloo et al. (2013) [31]	DI water	Transient hot wire method	Commercial	-	0.005–0.023	10–50	13.5	18
4	Maa et al. (2013) [32]	Silicone oil	Transient hot wire method	Custom built	-	0.004, 0.013, 0.022, 0.031	20–60	5.74	18.9
5	Kole et al.(2013) [33]	EG/Water(30/70)	Transient hot wire method	Custom built	Matrix-additive interface contact resistance of mis-oriented ellipsoidal particles	0.041–0.395	10–70	15	17
6	Ghozatloo et al. (2013) [34]	Ethylene glycol	Transient hot wire method	Commercial	-	0.1, 0.125, 0.15	30–40	21.2	-
7	Farid et al. (2015) [35]	Ethylene glycol	Transient hot wire method	Commercial	-	0.01, 0.02, 0.03	25–40	9	10.16
8	Amiri et al. (2015) [36]	DI water	Transient hot wire method	Commercial	Brownian motion and formation of surface nanolayer	0.011, 0.023, 0.045	20–50	18.96	28.125
9	Amiri et al. (2015) [37]	EG/water (40/60)	Transient hot wire method	Commercial	Brownian motion	0.0047, 0.0238, 0.0477, 0.0955	25–65	67.27	58.82
10	Arzani et al. (2015) [38]	DI water	Transient hot wire method	-	-	0.025, 0.05, 0.1	20–50	9.52	10.958
11	Sarsam et al. (2016) [39]	DI water	Transient hot wire method	Commercial	aspect ratio, differential effective medium (DEM)	0.011, 0.023, 0.034, 0.045	20–40	15.51	25
12	Mehrali et al. (2016) [40]	DI water	Transient hot wire method	Commercial	-	1–4	15–40	12.28	47.54
13	Yarmand et al. (2016) [41]	DI water	Transient hot wire method	Commercial	-	0.0091, 0.0272, 0.045	20–40	13.56	15.87
14	Agromayor et al. (2016) [42]	DI water	Transient hot wire method	Commercial	-	0.25, 0.5, 0.75, 1	20–40	11.66	12.69
15	Solangi et al. (2016) [43]	Propylene glycol treated water	Transient hot wire method	Commercial	-	0.025, 0.05, 0.075, 0.1	25–50	24.13	32.81
16	Sadri et al. (2017) [44]	DI water	Transient hot wire method	-	Brownian motion	0.05	20–45	15.51	24.18

Table 7. *Cont.*

S. No.	Author/Year	Base Fluid	Measurement Technique	Type	Mechanism	Vol% Range	Temperature Range (°C)	Enhancement (%) at Room Temp	Enhancement (%) at High Temp
17	Amiri et al. (2017) [45]	DI water	Transient hot wire method	Commercial	-	0.000455, 0.00091	20–50	18.64	22.58
18	Amiri et al. (2017) [46]	Transformer oil	Transient hot wire method	Commercial	-	0.0041	30–70	4	10
19	Esfahani et al. (2017) [47]	DI water	Transient hot wire method	Commercial	-	0.00455, 0.045	25–40	8.7	18.9
20	Jyothirmayee et al. (2011) [48]	EG/DI water	Transient hot wire method	Commercial	Shape effect and size effect of the nanoparticle.	0.004, 0.00275, 0.0415, 0.055, 0.07	25–50	2.4 6.5	17 36.1
21	Yu et al. (2011) [49]	Ethylene glycol	Transient hot wire method	Custom built	effect of 2D structure and stiffness	2, 5	10–60	84.18	86
22	Wanga et al. (2012) [51]	Oil	Transient hot wire method	Commercial	clustering effect of nanoparti-cles	0.17, 0.34, 0.18, 1.36	30–60	36	34
23	Ghozatloo et al. (2014) [57]	DI water	Transient hot wire method	Commercial	-	0.0023, 0.032, 0.045	10–60	29.2	32.81
24	Liuet al. (2014) [62]	Ionic liquid 1-hexyl-3-methylimidazolium tetrafluoroborate	Transient hot wire method	Custom built	-	0.0062, 0.0187, 0.0374	25–200	16.96	25.49
25	Sadaghinezhad et al. (2014) [64]	DI water	Transient hot wire method	Commercial	-	0.011, 0.0227, 0.034, 0.0454	15–40	18.96	23.80
26	Zanjani et al. (2014) [65]	DI water	Transient hot wire method	Commercial	-	0.005, 0.01, 0.02	25–45	5.8	10.3
27	Sadaghinezhad et al. (2015) [67]	DI water	Transient hot wire method	Commercial	-	0.0113, 0.0227, 0.034, 0.045	15–40	18.96	23.80
28	Mehrali et al. (2015) [70]	DI water	Transient hot wire method	Commercial	-	0.0113, 0.0227, 0.034, 0.045	15–40	11.94	27.67
29	Mehraliet al. (2015) [71]	DI water	Transient hot wire method	Commercial	-	0.0113, 0.0227, 0.034, 0.045	15–40	25.86	29.03
30	Ijam et al. (2015) [72]	DI water +EG(60:40)	Transient hot wire method	Commercial	-	0.0047–0.047	20–45	6.66	10.47
31	Kamatchi et al. (2015) [74]	DI water	Transient hot wire method	Commercial	Brownian motion	0.01, 0.1, 0.3 g/L	35–75	2.4	12.48
32	Askari et al. (2016) [76]	DI water	Transient hot wire method	Commercial	-	0.045	25–45	5	16
33	Esfahani et al. (2016) [77]	DI water	Transient hot wire method	Commercial	-	0.0045–0.227	25–60	20	56
34	Iranmanesh et al. (2016) [79]	DI water	Transient hot wire method	Commercial	Flagging of the inter-molecular adhesion forces	0.0227, 0.0341, 0.045	20–60	5.08	8.196
35	Naghash et al. (2016) [80]	DI water	Transient hot wire method	Commercial	-	0.045	15–40	1.11	1.18
36	Tahani et al. (2016) [81]	DI water	Transient hot wire method	Commercial	-	0.001, 0.005, 0.015, 0.045	25–50	1.17	11.47
37	Zanjani et al. (2016) [83]	DI water	Transient hot wire method	Commercial	-	0.005, 0.01, 0.02	25–45	5.88	9.52
38	Vakili et al. (2016) [85]	DI water	Transient hot wire method	Commercial	-	0.000113, 0.00022, 0.00045, 0.0022	25–50	5.172	15
39	Sarsam et al. (2016) [86]	DI water	Transient hot wire method	Commercial	-	0.045	20–40	6.89	11.475
40	Tharayil et al.(2016) [87]	DI water	Transient hot wire method	Commercial	-	0.003, 0.006, 0.009	-	-	27.6

Table 7. *Cont.*

S. No.	Author/Year	Base Fluid	Measurement Technique	Type	Mechanism	Vol% Range	Temperature Range (°C)	Enhancement (%) at Room Temp	Enhancement (%) at High Temp
41	Khosrojerdi et al. (2016) [88]	DI water	Transient hot wire method	Commercial	Brownian motion of the nanoplatelets	0.000113, 0.000227, 0.00045, 0.0022	25–50	5.128	9.682
42	Ahammed et al.(2016) [89]	DI water	Transient hot wire method	Custom built	Molecular collision and diffusion	0.05, 0.1, 0.15	10–50	20.68	28.02
43	Agarwalet al. (2016) [90]	Kerosene	Transient hot wire method	Commercial	-	0.0022, 0.0227, 0.09	20–70	19.6	26.21
44	Goodarzi et al. (2016) [91]	DI water	Transient hot wire method	Commercial	-	0.01, 0.02, 0.04, 0.06	20–60	6.61	10.025
45	Ranjbarzadeh et al. (2017) [93]	DI water	Transient hot wire method	-	Brownian motion	0.025, 0.05, 0.075, 0.1	30	30.979	-
46	Chen et al. (2017) [98]	DI water	Transient hot wire method	Custom built	-	0.001, 0.005, 0.01, 0.02, 0.05, 0.1	30–80	20.83	42.307
47	Iranmanesh et al. (2017) [99]	DI water	Transient hot wire method	Commercial	-	0.0113, 0.00227, 0.034, 0.045	15–70	26.315	36.36
48	Wang et al. (2017) [100]	WD type synthetic oil	Transient hot wire method	Commercial	-	0.02, 0.05, 0.2 mg/mL	30	25	-
49	Chai at al. (2017) [101]	Hydrogenated oil	Transient hot wire method	Commercial	-	25, 50, 100 ppm	30–50	-	14.4
50	Selvam et al. (2016) [104]	Ethylene glycol and water	Transient hot wire method	Commercial	High aspect ratio, two-dimensional geometry, stiffness	0.1, 0.2, 0.3, 0.4, 0.5	30–50	20.8416.04	-
51	Selvam et al. (2017) [105]	EG/Water (30/70)	Transient hot wire method	Commercial	Two-dimensional network and particle clustering of the nanoplatelets.	0.1, 0.2, 0.3, 0.4, 0.5	30–50	14.89	31.25
52	Selvam et al. (2017) [106]	EG/Water (30/70)	Transient hot wire method	Commercial	Two-dimensional network and particle clustering of the nanoplatelets.	0.001, 0.01, 0.05, 0.1, 0.15, 0.3, 0.45	30–50	18	-
53	Selvam et al. (2017) [107]	EG/Water (30/70)	Transient hot wire method	Commercial	Higher thermal conductive 2Dstructure of nanoplatelets and particle clustering, Brownian motion and micro-convection	0.1, 0.2, 0.3, 0.4, 0.5	30–50	-	29
54	Shaji et al. (2019) [109]	DI water	Transient hot wire method	Commercial	nano-size of GnP and the 2D geometry of the GnP	0.1, 0.2, 0.3, 0.4, 0.5	-10–40	23.78	23.46
54	Vishnuprasad et al. (2019) [110]	DI water	Transient hot wire method	Commercial	Brownian motion, high thermalcon-ductivity of GnP	0.025–0.5	28–70	55.38	-
54	Saeed et al. (2019) [111]	Propylene glycol	Transient hot wire method	Commercial	-	0.237, 0.475, 0.715, 0.956, 1.441.	50	51.8	-

Table 7. *Cont.*

S. No.	Author/Year	Base Fluid	Measurement Technique	Type	Mechanism	Vol% Range	Temperature Range (°C)	Enhancement (%) at Room Temp	Enhancement (%) at High Temp
55	Das et al. (2019) [112]	DI water	Transient hot wire method	Commercial	Brownian motion and conduction electrons at higher energy levels	0.009, 0.018, 0.027, 0.036, 0.045	25–45	17	29
56	Balaji et al. (2020) [113]	DI water	Transient hot wire method	Commercial	GnP size and the 2D geometry of the GnP	0.01, 0.05, 0.1, 0.15, 0.2	20–50	5	11

3.2. Density of Graphene Based Nanofluids

Arzani et al. (2015) [38] measured density using the weighing balance method for Deionized water-based graphene nanofluids at various volume fractions., viz., 0.025, 0.05, 0.1% and found a 0.4% increase in density at 0.1% vol fraction. Yarmand et al. (2016) [41] used Metlertoledo density meter for the measurement of density values for 0.0091, 0.0272, 0.045 vol% of graphene distilled water nanofluids and reported a 0.06% increase in the density value at 0.045 vol%. Sadri et al. (2017) [44] found 0.1% increase in the density value at 0.05 vol% of deionized water-based graphene nanofluids. Amiri et al. (2017) [45] used a metler Toledo density meter for the measurement of the density values for 0.001 and 0.002 vol% of graphene water nanofluids and found the increment of density values as less than 0.1%. Askari et al. (2016) [76] used pycnometer for the measurement of the density values for 0.045 vol% of graphene water nanofluids and reported a 0.73% increase in the density value at 0.045 vol%.

Amiri et al. (2015) [37] measured the density of graphene dispersed ethylene glycol water mixture (40/60) using the weighing balance method and found a 0.45% increase in the density at 0.0955 vol% of the nanoparticles. Solangi et al. (2016) [43] have reported the maximum increase in density as 4.5% at 0.1 vol% of graphene dispersed propylene glycol treated water nanofluids. Liuet al. (2014) [62] observed an increment of about 3.66% for 0.0374 vol% of graphene nanoplatelets dispersed in ionic liquid 1-hexyl-3-methylimidazolium tetrafluoroborate respectively. Ijam et al. (2015) [72] measured the density of graphene dispersed ethylene glycol water mixture (40/60) using a density meter (DA130N) and found 1.14% increase in the density at 0.045 vol% of the nanoparticles. Selvam et al. (2017) [105,107] measured the density values for graphene dispersed in ethylene glycol water mixture (30/70) respectively and reported a 4% enhancement in the density at 0.5 vol% of nanoplatelets in the base fluid. The percentage increase in density is minimal and sometimes insignificant due to the less bulk desnity of GnP (2.2 g/cc).

A summary of the published literature on density of graphene-based nanofluids has been provided in Table 8. Published literature reveals increase in density of the nanofluids is due to the higher density of the GnP. The density increases with increase in GnP loading. However, the increment is seen lower as compared with the metal and metal oxide dispersed nanofluids due to the lesser density of GnP. Decrease in the density of the nanofluids was seen with increase in temperature due to the increased intermolecular distance between the nanofluid molecules.

Table 8. Summary of published literature on density of graphene-based nanofluids.

S. No.	Author/Year	Base Fluid	Measurement Technique	Vol%	Results
1	Amiri et al. (2015) [37]	EG/water (40/60)	Weighing balance method	0.0047, 0.0238, 0.0477, 0.0955	Decreases by 2.8% and 2.5% at 25 °C and 65 °C
2	Arzani et al. (2015) [38]	DI water	Weighing balance method	0.025, 0.05, 0.1	Increases by 0.4% at 0.1%

Table 8. *Cont.*

S. No.	Author/Year	Base Fluid	Measurement Technique	Vol%	Results
3	Yarmand et al. (2016) [41]	DI water	Metler Toledo DE40 density meter	0.0091, 0.0272, 0.045	Increases by 0.06% for 0.1% at 40 °C
4	Solangi et al. (2016) [43]	Propylene glycol treated water	Not reported	0.025, 0.05, 0.075, 0.1	Increases by 4.5% at 0.1 vol%
5	Sadri et al. (2017) [44]	DI water	Not reported	0.05	Increases by 0.1% at 0.05 vol%
6	Amiri et al. (2017) [45]	DI water	Metler Toledo DE40 density meter	0.001, 0.002	Increases with less than 0.1% at 0.002 vol%
7	Liuet al. (2014) [62]	Ionic liquid 1-hexyl-3-methylimidazolium tetrafluoroborate	Weighing balance method	0.0062, 0.0187, 0.0374	Increases by 3.66% at 0.0374 vol%
8	Ijam et al. (2015) [72]	DI water +EG(60:40)	Density meter (DA 130N)	0.0047–0.047	Decreases by 1.14% on 0.045 vol%
9	Askari et al. (2016) [76]	DI water	Pycnometer	0.045	Increases by 0.73% on 0.045 vol%
10	Selvam et al. (2017) [105]	EG/Water (30/70)	Weighing balance method	0.1, 0.2, 0.3, 0.4, 0.5	Increases by 4% at 0.5 vol%
11	Selvam et al. (2017) [107]	EG/Water (30/70)	Weighing balance method	0.1, 0.2, 0.3, 0.4, 0.5	Density ratio increases from 1.029 to 1.049

3.3. Rheological Characteristics of Graphene Based Nanofluids

Much research has been conducted for the prediction of the rheological behavior of aqueous graphene dispersed nanofluids. Amiri et al. [36] measured the rhelogical properties of deionized water-based graphene nanofluids in the range of 0.011, 0.023, 0.045 vol% using a Brook field rheometer (DVIII Ultra Rheometer) with shear rate of 300 s^{-1} and reported a 29.4% increase in viscosity at 0.045 vol%. Sarsam et al. (2016) [39] used a Anton Paar rotational rheometer for the measurement of the viscosity of distilled water-based graphene nanofluids at the shear rate of 20–200 1/s and reported a 15.29% increase in the viscosity at 0.045 vol%. Yarmand et al. (2016) [41] have reported an enhancement of about 24% when measuring the viscosity of distilled water-based graphene nanofluids of concentration in the range of 0.0091, 0.0272, 0.045 vol% using an Anton Paar rheometer at the shear rate of 500 s^{-1}. Agromayor et al. (2016) [42] observed a remarkable increase in viscosity when measuring with Physica MCR 101 rheometer respectively. Amiri et al. (2017) [45] used Anton Paar rotational rheometer at the shear rate of 20–300 s^{-1} for water-based graphene nanofluids and found a 3.58% increase in the viscosity for 0.00091 vol%. Esfahani et al. (2017) [47] used a AR 500 rheometer for the measurement of the viscosity of deionized water-based graphene nanofluids of 0.0045 vol%, 0.045 vol% respectively at the shear rate of 10–100 s^{-1} and found a 60% enhancement in the viscosity at 0.045 vol% respectively. Sadeghinezhad et al. (2014) [64], Sadeghinezhad et al. [67] &Mehrali et al. [70], Mehrali et al. [71] studied the rheological characteristics of GnP-H_2O nanofluid at 500 s^{-1} shear rate and have reported an increase in the viscosity with the addition of GnP in the water. The viscosity of nanofluid decreased from 9–38% when the temperature increased from 15–55 °C. Esfahani et al. (2016) [77] observed an enhancement of about 130% when measuring the viscosity of deionized water-based graphene nanofluids using AR 500 rheometer at the shear rate of 100 s^{-1} respectively. Iranmanesh et al. (2016) [79] used a Anton Paar rheometer for the measurement of the viscosity of distilled water-based graphene nanofluids with concentrations varying from 0.0227, 0.0341, 0.045 vol% and

reported an enhancement of about 20.83% respectively. Sarsam et al. (2016) [86] studied the rheological characteristics of distilled water-based graphene nanofluids using a rotational rheometer for the concentration of 0.045 vol% and reported a 20.83% enhancement in the viscosity. Goodarzi et al. (2016) [91] measured the rheological properties of deionized water-based graphene nanofluids in the range of 0.01%, 0.02%, 0.04% and 0.06% using Anton Paar rheometer and reported a 3.78% increase in viscosity at 0.06vol% respectively. Vakili et al. (2017) [92] measured the viscosity of deionized water-based graphene nanofluids with concentration varying from 0.0113–0.045 vol% using an Anton Paar rheometer and reported a 32% increase in the viscosity at 0.045 vol%. Iranmanesh et al. (2017) [99] used an Anton Paar rotational rheometer for the measurement of the viscosity of distilled water-based graphene nanofluids and reported a 23% increase in the viscosity at 0.045 vol%.

Ma et al. (2013) [32] studied the rheological characteristics of silicone oil based graphene nanofluids using a ARG 2 Rheometer for concentrations varying from 0.004–0.031 vol% and reported a 48.11% decrease in viscosity with increasing temperature. Amiri et al. (2015) [37] measured the viscosity of Ethylene Glycol/water (40/60) based graphene nanofluids with concentrations varying from 0.0047, 0.0238, 0.0477, 0.0955 vol% using a Brook field rheometer (DVIII Ultra Rheometer) at the shear rate of 140 s^{-1} and reported a 1.94% increase in viscosity at 0.0955 vol%. Amiri et al. (2017) [46] used transformer oil based graphene nanofluids of 0.0041 vol% and measured the viscosity using a Brookfield LVDV-III rheometer and reported an approximate 1.3% enhancement in viscosity. Wanga et al. (2012) [51] used a rheometer for the measurement of the viscosity of oil based graphene nanofluids at the shear rate of 0.1 to 1000 s^{-1} and reported 1.36 vol% nanofluids exhibiting pseudoplastic fluid behavior and slight visco elasticity enhancement. Ijam et al. [72] studied the rheology behavior of GNP/H_2O-EG nanofluid through variation in the shear rate from 0.1 to 1000 s^{-1} containing 0.0047–0.047 vol% of GnP. Authors reported shear thinning behavior for GnP/H_2O-EG nanofluid at a low shear rate while Newtonian behavior was observed under higher shear rate. Viscosity increased up to 35% for 0.045 vol% at 20 °C. A 48% decrease in viscosity was seen when the temperature increased from 20 to 60 °C at 0.047 vol% of GnP. Chai et al. (2017) [101] studied the rheology behavior of GNP/ hydrogenated oil nanofluid through variation in the shear rate from 0 to 140 s^{-1} containing 25–100 ppm of GnP. They have reported the shear thinning behavior for GnP/H_2O-EG nanofluid at low shear rate while Newtonian behavior was observed at a higher shear rate. Viscosity increased up to 54% for higher concentrations respectively. Saaed et al. (2019) [111] studied the rheology behavior of GnP/Propylene glycol nanofluid through variation in the shear rate from 0 to 1000 s^{-1} and observed enhancement in viscosity on GnP loading and decrement with increase in temperature. Prabakaran et al. (2019) [133,134] studied the rheology behavior of GnP/PCM nanofluid through variation in the shear rate from 0 to 1000 s^{-1} and observed a 1180% enhancement in the viscosity at a lower shear rate while the viscosity enhanced only by 57.7% at a higher shear rate respectively at the temperature of 30 °C. At the temperature range of 20 °C, the increase in the viscosity was found to be only 37% due to the addition of GnP. Balaji et al. (2020) [113] studied the rheological behavior of GnP dispersed deionized water nanofluids and found a 13% increase in viscosity with the addition of GnP into the base fluid.

Studies relating to the rheological behavior of GnP nanofluids are rather limited. Several researchers have reported an increase in the viscosity of the GnP nanofluids with GnP loading and a decrease with increase in temperature seen as in direct relationship with the density of the nanofluids. The significant increment in viscosity will have a direct effect on heat transfer coefficient and pumping power of thermal systems. The higher mass flow rate causes more convection and thinner boundary layer is formed which enhances the heat transfer. For a fixed mass flow rate, as particle volume fraction increases the heat transfer coefficient increases even though the Reynolds number decreases (viscosity increases). The enhancement in thermal conductivity was higher than the increment in viscosity which in turn the enhancement in the heat transfer. Some researchers have reported Newtonian and non-Newtonian behavior of the GnP nanofluids at different shear rates. GnP loading was

seen causing changes in the Newtonian behavior of nanofluids into non-Newtonian fluids. However, the nanofluids obeyed the Newton's law of viscosity with increasing shear rate.

A summary of the published literature on rheological characteristics of graphene-based nanofluids has been provided in Table 9.

Table 9. Summary of published literature on rheological characteristics of graphene-based nanofluids.

S. No.	Author	Base fluid	Measurement Technique	Vol% Range	Shear Rate Range	Results
1	Ma et al. (2013) [32]	Silicone oil	ARG 2 Rheometer	0.004, 0.013, 0.022, 0.031	1 s^{-1}	Viscosity decreases by 48.11% with increasing temperature
2	Amiri et al. (2015) [36]	DI water	Brook field rheometer (DVIII Ultra Rheometer)	0.011, 0.023, 0.045	300 s^{-1}	Viscosity increases by 29.4% at 0.1 vol%
3	Amiri et al. (2015) [37]	EG/water (40/60)	Brook field rheometer (DVIII Ultra Rheometer)	0.0047, 0.0238, 0.0477, 0.0955	140 s^{-1}	Viscosity increases by 1.94% at 0.0955 vol%
4	Sarsam et al. (2016) [39]	DI water	Anton Paar rheometer	0.011, 0.023, 0.034, 0.045	20–200 s^{-1}	Viscosity increases by 15.29% at 0.045 vol%
5	Yarmand et al. (2016) [41]	DI water	Anton Paar rheometer	0.0091, 0.0272, 0.045	500 s^{-1}	Increases by 24% at 0.1 vol%
6	Agromayor et al. (2016) [42]	DI water	Physica MCR 101 rheometer (Anton Paar, Graz, Austria	0.25, 0.5, 0.75, 1	-	Remarkable increase in viscosity was observed.
7	Amiri et al. (2017) [45]	DI water	Anton Paar rheometer (model Physica MCR301, Anton Paar GmbH)	0.000455, 0.00091	20–300 s^{-1}	Enhances by 3.58% for 0.00091 vol%
8	Amiri et al. (2017) [46]	Transformer oil	Brookfield LVDV-III rheometer	0.0041	-	Emhances by 1.3% on GnP loading
9	Esfahani et al. (2017) [47]	DI Water	AR 500 rheometer	0.00455, 0.045	10–100 s^{-1}	Maximum enhancement was found to be 60% at 0.045 vol%
10	Wanga et al. (2012) [51]	Oil	HAAKE RS6000 (Germany) Rheometer	0.17, 0.34, 0.18, 1.36	0.1 to 1000 s^{-1}	pseudoplastic fluid behaviors of obvious shear thinning, viscosity increase, and slight viscoelasticity enhancement for the 1.36 vol.%.
11	Sadaghinezhad et al. (2014) [64]	DI water	Anton Paar rheometer	0.011, 0.0227, 0.034, 0.0454	500 s^{-1}	Viscosity decreases by 9 to 38% at increasing temperature
12	Sadeghinezhad et al. (2015) [67]	DI water	Anton Paar rheometer	0.0113, 0.0227, 0.034, 0.045	500 s^{-1}	Viscosity decreases by 9 to 38% at increasing temperature

Table 9. *Cont.*

S. No.	Author	Base fluid	Measurement Technique	Vol% Range	Shear Rate Range	Results
13	Mehrali et al. (2015) [70]	DI water	Anton Paar rheometer	0.0113, 0.0227, 0.034, 0.045	500 s^{-1}	Viscosity decreases by 9 to 38% at increasing temperature
14	Mehrali et al. (2015) [71]	DI water	Anton Paar rheometer	0.0113, 0.0227, 0.034, 0.045	500 s^{-1}	Viscosity decreases by 9 to 38% at increasing temperature
15	Ijam et al. (2015) [72]	H_2O:EG (60:40)	Anton Paar rheometer	0.0047–0.047	0.1 to 1000 s^{-1}	Shear thinning behavior was observed for GNP/H_2O-EG nanofluid at low shear rate while Newtonian behaviour was observed under higher shear rate.
16	Esfahani et al. (2016) [77]	DI water	AR 500 rheometer	0.0045–0.227	100 s^{-1}	Maximum enhancement in viscosity was found to be 130%
17	Iranmanesh et al. (2016) [79]	DI water	Anton Paar rheometer, Austria	0.0227, 0.0341, 0.045	-	Enhancement was found to be 20.83%
18	Sarsam et al. (2016) [86]	DI water	Anton Paar rheometer (model Physica MCR 301, GmbH)	0.045	20–200 s^{-1}	Enhancement was found to be 20.83%
19	Goodarzi et al. (2016) [91]	DI water	Anton Paar rheometer (Physica MCR 302)	0.01, 0.02, 0.04, 0.06	-	Enhancement was found to be 3.78%
20	Vakili et al. (2017) [92]	DI water	Anton Paar rheometer (Physica MCR 301, GmbH, Graz, Austria	0.0113, 0.00227, 0.034, 0.045	-	Enhancement was found to be 32%
21	Iranmanesh et al. (2017) [99]	DI water	Anton Paar rheometer (Physica MCR 301,GmbH, Graz, Austria	0.0113, 0.00227, 0.034, 0.045	-	Enhancement was found to be 23%
22	Chai et al. (2017) [101]	Hydrogenated oil	Malvern Bohlin Gemini II Rheometer	25ppm, 50ppm, 100ppm	0 to 140 s^{-1}	Enhancement was found to be 54%
23	Saaed et al. (2017) [111]	Propylene glycol	Anton Paar rheometer (Physica MCR 101)	0.237, 0.475, 0.715, 0.956, 1.441.	0 to1000 s^{-1}	Shear thinning behaviour was observed for GnP nanofluid at low shear rate while Newtonian behaviour was observed at higher shear rate.
24	Das et al. (2017) [112]	DI water	Anton Paar rheometer (Physica MCR 101)	0.009, 0.018, 0.027, 0.036, 0.045	0 to1000 s^{-1}	Enhances by 175% at 0.1wt%
25	Prabakaran et al. (2018) [133]	OM08-Fatty acid mixture	Anton Paar rheometer	0.1, 0.2, 0.3, 0.4, 0.5	0 to 1000 s^{-1}	At 30 °C, Increases by 57.7% at 0.5 vol% at 1000s^{-1} and 1180% at 1 s^{-1}

Table 9. *Cont.*

S. No.	Author	Base fluid	Measurement Technique	Vol% Range	Shear Rate Range	Results
26	Prabakaran et al. (2018) [134]	OM08-Fatty acid mixture	Anton Paar rheometer	0.1, 0.2, 0.3, 0.4, 0.5	0 to 1000 s^{-1}	Increases by 37% at 20 °C
27	Balaji et al. (2020) [113]	DI water	Anton Paar rheometer	0.01, 0.05, 0.1, 0.15, 0.2	0 to 1000 s^{-1}	Increases by 13.3% at 20 °C

3.4. Specific Heat Capacity of Graphene Based Nanofluids

Arzani et al. (2015) [38] measured the specific heat for deionized water-based graphene nanofluids at various volume fractions., viz., 0.025, 0.05, 0.1% and found a 3.03% decrease in specific heat at 0.1 vol% fraction. Mehrali et al. (2016) [40] have made theoretical prediction of the specific heat values of distilled water-based graphene nanofluids and reported a 35.2% decrease in specific heat at 4% volume fraction. Yarmand et al. (2016) [41] used Differential scanning calorimeter (DSC 8000) for the measurement of the specific heat values for 0.0091, 0.0272, 0.045 vol% of graphene distilled water nanofluids and reported a 6.09% decrease in the specific heat value at 0.045 vol%. Agromayor et al. (2016) [42] determined the specific heat values for graphene water nanofluids using a differential scanning calorimeter and reported a 0.8% decrease in the specific heat value at 1 vol%. Sadri et al. (2017) [44] found a 1.69% decrease in specific heat value for 0.05 vol% of deionized water-based graphene nanofluids. Goodarzi et al. (2016) [91] calculated the specific heat for graphene water nanofluids and found a 8.78% decfease in specific heat value for 0.06 vol% at 20 °C. Chen et al. (2017) [98] used a differential scanning calorimeter for the measurement of specific heat values and reported a 5.43% decrease in specific heat at 0.1 vol% of graphene in water. Iranmanesh et al. (2017) [99] measured the specific heat values for 0.045 vol% of graphene water nanofluids and reported a 10.61% decrease in specific heat value at 0.045 vol%.

Ghozatloo et al. (2013) [34] used theoretical predictions of xuan and roetzal equations in their estimation of the specific heat of graphene dispersed ethylene glycol nanofluids for volume fractions viz., 0.1, 0.125, 0.15% respectively and found the maximum decrease in specific heat as 18.9% at higher volume concentrations. Amiri et al. (2015) [37] measured the specific heat of graphene dispersed ethylene glycol water mixture (40/60) using a differential scanning calorimeter and found a 5% decrease in specific heat at 0.096 vol% of the nanoplatelets. Solangi et al. (2016) [43] have reported the maximum decrease in specific heat as 24.6% at 0.1 vol% of graphene dispersed propylene glycol treated water nanofluids. Ghozatloo et al. (2014) [57] have predicted the specific heat values using theoretical equations and found a 11.97% increase in values at 0.045 vol%. Liu et al. (2014) [62] observed a decrement of about 24% for 0.0374 vol% of graphene nanoplatelets dispersed in ionic liquid 1-hexyl-3-methylimidazolium tetrafluoroborate respectively. Ijam et al. (2015) [72] measured the specific heat of graphene dispersed ethylene glycol water mixture (40/60) using a differential scanning calorimeter (4000) and found a 9.05% decrease in the specific heat at 0.045 vol% of the nanoplatelets.

Selvam et al. (2017) [105] measured the specific heat values for graphene dispersed in ethylene glycol water mixture (30/70) respectively and reported a 9% decrease in the specific heat at 0.5 vol% of nanoplatelets in the base fluid. Selvam et al. (2017) [106,107] again reported decrement in specific heat of about 8% for 0.15 vol% fraction of graphene in ethylene glycol water mixture (30/70) respectively.

A summary of the published literature on specific heat capacity of graphene-based nanofluids has been provided in Table 10.

Table 10. Summary of published literature on specific heat capacity of graphene-based nanofluids.

S. No.	Author/Year	Base Fluid	Measurement Technique	Vol Range	Increment/Decrement
1	Ghozatloo et al. (2013) [34]	Ethylene glycol	Xuan and roetzal equation Analytical prediction	0.1, 0.125, 0.15	Decreases by 18.9%
2	Amiri et al. (2015) [37]	Ethylene Glycol/water (40/60)	Differential scanning calorimeter	0.0047, 0.0238, 0.0477, 0.0955	Decreases by 5%
3	Arzani et al. (2015) [38]	DI water	Not reported	0.025, 0.05, 0.1	Decreases by 3.03%
4	Mehrali et al. (2016) [40]	DI water	Rule of mixtures Analytical prediction	1–4	Decreases by 35.2%
5	Yarmand et al. (2016) [41]	DI water	Differential scanning calorimeter (DSC 8000)	0.0091, 0.0272, 0.045	Decreases by 6.09%
6	Agromayor et al. (2016) [42]	DI water	Differential scanning calorimeter (Q,2000)	0.25, 0.5, 0.75, 1	Decreases by 0.8%
7	Solangi et al. (2016) [43]	Propylene glycol treated water	Differential scanning calorimeter	0.025, 0.05, 0.075, 0.1	Decreases by 24.6%
8	Sadri et al. (2017) [44]	DI water	Differential scanning calorimeter	0.05	Decreases by 1.69%
9	Ghozatloo et al. (2014) [57]	DI water	Rule of mixtures Analytical prediction	0.004, 0.00275, 0.0415, 0.055, 0.07	Increases by 11.97%
10	Liuet al. (2014) [62]	ionic liquid 1-hexyl-3-methylimidazolium tetrafluoroborate	Differential scanning calorimeter (Q,20)	0.0062, 0.0187, 0.0374	Decreases by 24%
11	Ijam et al. (2015) [72]	DI water + EG(60:40)	Differential scanning calorimeter (4000)	0.0047–0.047	Decreases by 9.05%
12	Goodarzi et al. (2016) [91]	DI water	Not reported	0.01, 0.02, 0.04, 0.06	Decreases by 8.78%
13	Chen et al. (2017) [98]	DI water	Differential scanning calorimeter (Q,20)	0.001, 0.005, 0.01, 0.02, 0.05, 0.1	Decreases by 5.43%
14	Iranmanesh et al. (2017) [99]	DI water	Not reported	0.0113, 0.00227, 0.034, 0.045	Decreases by 10.61%
15	Selvam et al. (2017) [105]	EG/Water (30/70)	Differential scanning calorimeter	0.1, 0.2, 0.3, 0.4, 0.5	Decreases by 9%
16	Selvam et al. (2017) [106]	EG/Water (30/70)	Differential scanning calorimeter	0.001, 0.01, 0.05, 0.1, 0.15, 0.3, 0.45	Decreases by 8%
17	Selvam et al. (2017) [107]	EG/Water (30:70)	Differential scanning calorimeter	0.1, 0.2, 0.3, 0.4, 0.5	Decreases by 9%

The inference from readings from literature provided above is that the specific heat capacity of the nanofluids decreases with GnP loading. This is due to the specific heat capacity of the GnP being much lower compared with the base fluids and hence the addition of this low specific heat capacity nanomaterials to the base fluid will effectively cause a decrease in the specific heat capacity of the nanofluids. Decrease in the specific heat capacity of the nanofluids was seen with increase in temperature.

4. Convective Heat Transfer Characteristics of Graphene Nanofluids

All heat transfer applications must design the heat transfer types of equipment effectively and compactly in finding the heat transfer coefficient, ensuring enhancement in the heat transfer. Thus, the heat transfer fluids must possess a high convective heat transfer coefficient for better system performance. Many researchers have reported convective behavior of graphene suspended nanofluids tested under different conditions and seen that the several factors as responsible for the better convective characteristics of the nanofluids.

4.1. Convective Heat Transfer Characteristics of Aqueous Based Nanofluids with Graphene

Arzani et al. (2015) [38] conducted experiments on deionized water-based graphene nanofluids in an annular tube with a Reynolds number 17,000 and found a 22% enhancement in the heat transfer coefficient at 0.045 vol% with a corresponding pressure drop of 2.250 kPa respectively. Mehrali et al. (2016) [40] found an enhancement of about 27% in 'h'at 4% with 0.62 kPa pressure drop for distilled water/graphene nanofluids. Yarmand et al. (2016) [41] conducted experiments on graphene/distilled water nanofluids in a stainless steel square pipe of following dimensions., 1.4 m length, 10 mm inner width, and 12.8 mm outer width, respectively with Reynolds number of 17,500 and reported a 19.68% enhancement in the heat transfer coefficient at 0.045 vol%. Agromayor et al. (2016) [42] tested the nanofluids in a stainless-steel tube in tube heat exchanger of dimensions 1180mm length, 10mm OD, 8mm ID and found a 32% enhancement in the 'h' at 0.5% with pressure drop of about 28kPa.

Ghozatloo et al. (2014) [57] tested the deionized water-based graphene nanofluids in a horizontal circular copper tube of dimensions 1 m length, 1.07 cm ID, 1.30 cm OD at Reynolds number of 1940 and saw a 23.9% enhancement in the 'h' at 0.045 vol%. Sadaghinezhad et al. (2014) [64] used a straight stainless steel tube of 1400 mm length, 12 mm OD, 10 mm ID as a test section in their study of the heat transfer characteristics of graphene/distilled water nanofluids and found a 160% enhancement in the 'h' at 0.045 vol% with the corresponding pressure drop of 3.6 kPa respectively. Zanjani et al. (2014) [65] dispersed graphene in a distilled water and flowed it through a uniformly heated copper tube of dimensions 2740.2 mm length, 4.2 mm ID, 6 mm OD at Reynolds number of 10,850 and reported a 6.04% enhancement in the 'h' at 0.02 vol% with a corresponding pressure drop of about 62.2 kPa. Sadaghinezhad et al. (2015) [67] dispersed graphene in a distilled water and conducted experiments in a straight stainless steel tubes of dimensions 1400 mm length, 12 mm OD, 10 mm ID at Reynolds number of 18,187 and found a 83% enhancement in the Nusselt number at 0.045 vol% with a corresponding pressure drop of 3.6 kPa. Mehrali et al. (2015) [70] found a 200% enhancement in 'h' at 0.045 vol% of graphene in deionized water when flowed through a straight stainless steel tube of dimensions 1400 mm length, 12 mm OD, 10 mm ID respectively. Mehrali et al. (2015) [71] conducted experiments on distilled water-based graphene nanofluids in a straight stainless steel tube of dimensions 2000 mm, 6.5 mm OD, 4.5 mm ID respectively and reported an enhancement up to 15% in the heat transfer coefficient at 0.045 vol% with a corresponding pressure drop of about 1.17 kPa.

Kim et al. (2016) [78] tested graphene nanofluids in a heat pipe and reported enhancement up to 25% in the value of 'h'at 0.03 vol%. Naghash et al. (2016) [80] dispersed graphene in a deionized water and made variations in the Reynolds number upto 6000 by allowing the nanofluid to flow through straight copper tube of 109 cm length, 11 mm ID and found a 34% enhancement in the value of 'h' at 0.1% respectively. Goodarzi et al. (2016) [91] made variations in the Reynolds number up to 15,000 by flowing the water-based graphene nanofluids in a Double pipe heat exchanger and found a 15.86% enhancement in the value of 'h' at 0.06%. Ranjbarzadeh et al. (2017) [93] observed a pressure drop of about 6.4 kPa with 'h' enhancement of about 40.3% at 0.1%of graphene in water when flowing through a copper tube of dimensions 8.5 mm ID and 10 mm OD respectively. Arshad et al. (2017) [103] used micro channel heat sink for testing the Deionized water-based graphene nanofluids and found that the value of 'h' enhances by 21.51%. Vishnuprasad et al. (2017) [110] used

aluminium water block for testing the Deionized water-based graphene nanofluids and found a 78.5% enhancement in the value of 'h' at 0.2 vol%.

4.2. Convective Heat Transfer Characteristics of Non-Aqueous Based Nanofluids with Graphene

Baby et al. (2011) [30] conducted experiments on deionized water and ethylene glycol based graphene-based nanofluids separately with the Reynolds number ranging at 15,500 and 1000 respectively in a straight stainless steel tube heated by copper wire and reported the 171% enhancement in the heat transfer coefficient at 0.01% and 219% at 0.01% for deionized water and ethylene glycol respectively. Ghozatloo et al. (2013) [34] dispersed graphene in ethylene glycol with Reynolds number of 2840 in a straight pipe subjected to a constant heat flux and found a 42.2% enhancement in the heat transfer coefficient at 0.15%. Amiri et al. (2015) [37] dispersed graphene in EG/water (40/60) and tested in a car radiator. The result was an enhancement of 'h' by 130% at 0.0955 vol% with corresponding pressure drop of 0.55 kPa inside the radiator tubes. Solangi et al. (2016) [43] conducted the experiments on propylene glycol treated water-based graphene nanofluids in straight seamless copper tube of dimensions, 1500 mm length, 8 mm OD, 4 mm ID at Reynolds number of 11,770 and concluded that the 'h' enhances by 119% at 0.1% respectively.

Amiri et al. (2017) [46] found an enhancement of about 32% in 'h'at 0.0041 vol% when dispersing graphene in a transformer oil. Zanjani et al. (2016) [83] used 2740.2 mm length, 4.2 mm ID, 6 mm OD uniformly heated copper tube as a test section with Reynolds number of 1760 and found a 14% enhancement in the heat transfer coefficient at 0.045 vol%. Agarwal et al. (2016) [90] dispersed graphene in a kerosene and tested its heat transfer characteristics in a long stainless steel tube of 12 m long, 9.5 mm OD, 0.9 mm thick with Reynolds number of 25,000 and found enhancement in 'h' was up to 45% at 0.09 vol% respectively.

Selvam et al. (2017) [105] dispersed graphene in EG/Water (30/70) and tested the nanofluids at a Reynolds number of 6790 in a tube in tube heat exchanger of dimensions 2.97 m, 10.5 mm OD, 4.3 mm ID and found the enhancement in 'h' as 170% at 0.5 vol% fraction with a corresponding pressure drop of about 59.13 kPa as shown in the Figure 6. The increase in volume concentration of GnP caused increase in the viscosity due to which the Reynolds number gets decreased. However, the reduced Reynolds number was restored by increasing mass flow rate. The increase in the mass flow rate was seen increasing the convective heat transfer coefficient. Particle aggregation was reported to be the major reason for increment in the heat transfer coefficient. At higher Reynolds number and higher GnP loading, the particle aggregation broke down due to collision with the tube walls resulting in a steep increase in the convective heat transfer coefficient, respectively. Increment in the convective heat transfer coefficient was higher for higher nanofluid inlet temperature due to the increment in thermal conductivity and decrement in viscosity at higher temperature of the nanofluids.

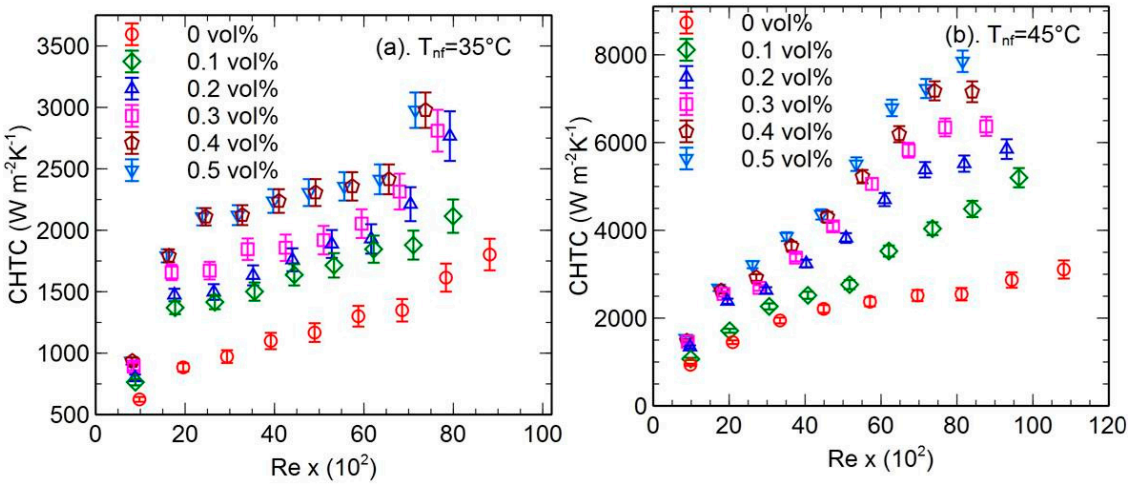

Figure 6. Variation of CHTC in a tube in tube heat exchanger [105].

Selvam et al. (2017) [107] tested the graphene nanofluids in an automobile radiator for the Reynolds number up to 250 and reported an 80% enhancement of heat transfer coefficient at 0.5 vol% of nanoplatelets. This is shown in the Figure 7. They have also reported that the enhancement in heat transfer coefficient could be due to the improved thermal conductivity of nanofluids, particle clustering, particle migration, and reduction of boundary layer thickness.

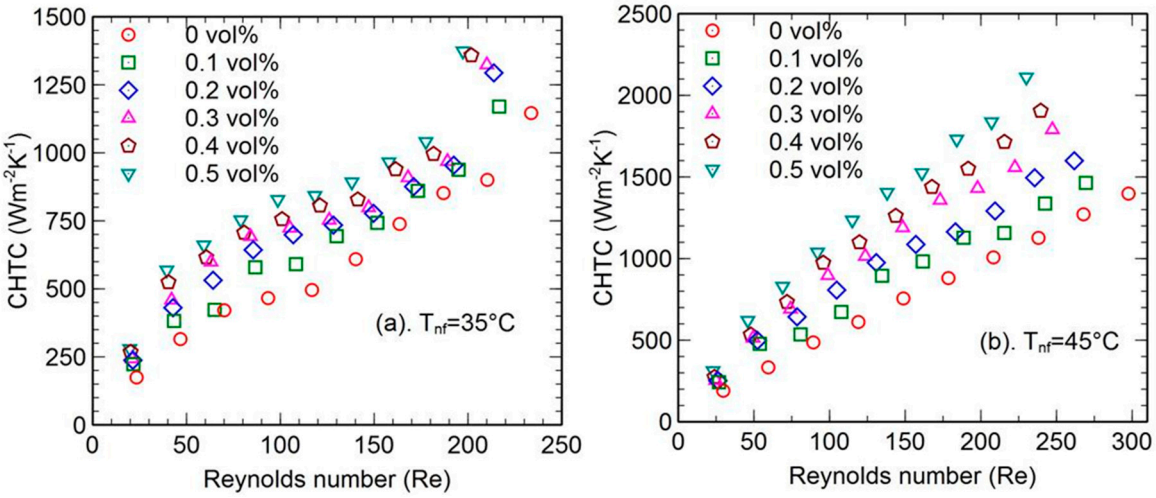

Figure 7. Variation of CHTC in automobile radiator [107].

Selvam et al. (2017) [108] made repeated experiments with the same nanofluids in an automobile radiator for different inlet velocity of the air to the radiator. Variations of OHTC with respect to Reynolds number at various fan inlet velocities and nanofluid concentration are shown in Figures 8 and 9. Increase in OHTC was seen with increase in Reynolds number and air velocity due to enhanced heat flux of air. Increment in the air velocity caused increase in the convection effects and the results showed a 50% maximum increment for every 1 m/s of air velocity. However, the maximum enhancement was found to be 125% at higher mass flow rate of the nanofluid and higher velocity of the air as compared with the lower velocity of air. The figure showed an enhancement in OHTC at higher temperature of the nanofluids at 45 °C compared with the nanofluids at the temperature of 35 °C. Balaji et al. (2020) [113] conducted experiments on copper microchannel heat sink by passing GnP-dispersed deionized water nanofluids at various heat loads ranging from 50 W to 200 W. There is an enhancement of 27.3% and 71% in the heat transfer coefficient at lower and higher heat flux, respectively.

A summary of the published literature on heat transfer characteristics of graphene-based nanofluids has been provided in Table 11. The inference is that the heat transfer coefficient increases following an increase in mass flow rate and the GnP loading in all the cases. At higher mass flow rate, the thermal boundary layer becomes thinner, and the convection effect increases which, in turn, results in the enhanced heat transfer. Another possible reason for the enhancement is the GnP loading. This is due to the fact that the higher thermal conductivity of the GnP and reduction in thermal boundary layer upon GnP loading causes enhanced heat transfer results in increased heat transfer coefficient. The random movement of the nanoparticles in the fluids, shape and size effect of the GnP, and particle clustering were reported to be the possible mechanisms for the increment in the thermal conductivity. Particle aggregation, Brownian motion and the viscosity gradient were reported to be the possible mechanisms for the decrement in the thermal boundary layer thickness. These overall mechanisms were found to constitute the reason for the enhancement in the convective heat transfer coefficient respectively. Several researchers have reported different significant enhancements of the heat transfer coefficient for GnP nanofluids under different applications. Particle aggregation was the cause of the enhancement at higher concentration of the nanoplatelets. At higher Reynolds number, the particle

aggregation breaks down resulting in steep increase of the heat transfer coefficient due to the collision of the particles with the side walls [105]. Some researchers have reported the coupling of high aspect ratio of GnP and the high thermal conductivity of GnP participates effectively in transferring energy between the fluid molecules and the side walls resulting in high heat transfer coefficient. However, several anomalies were existing in the mechanisms responsible for the increment in the heat transfer coefficient. Hence further research has to be made for finding the exact mechanisms responsible for the increment in the heat transfer coefficient for different flow areas especially at turbulent flow regions. However, this significant enhancement in the heat transfer coefficient could promote the graphene nanofluids for heat transfer applications replacing the conventional coolants which could in turn make the thermal systems compact.

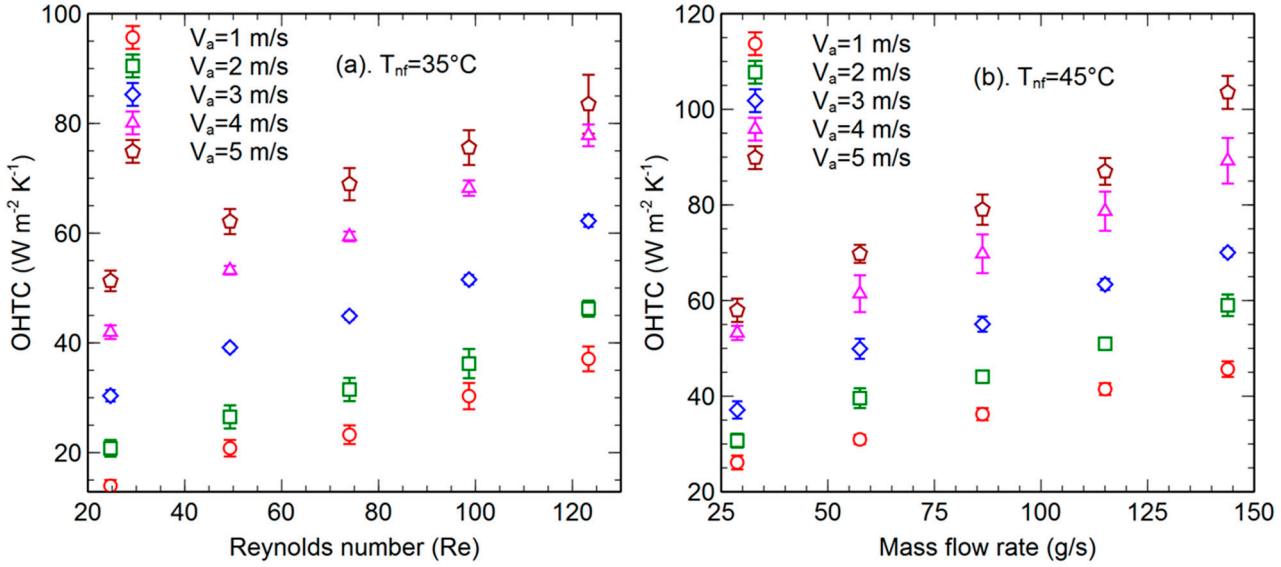

Figure 8. Variation of OHTC in an automobile radiator for various fan velocities [108].

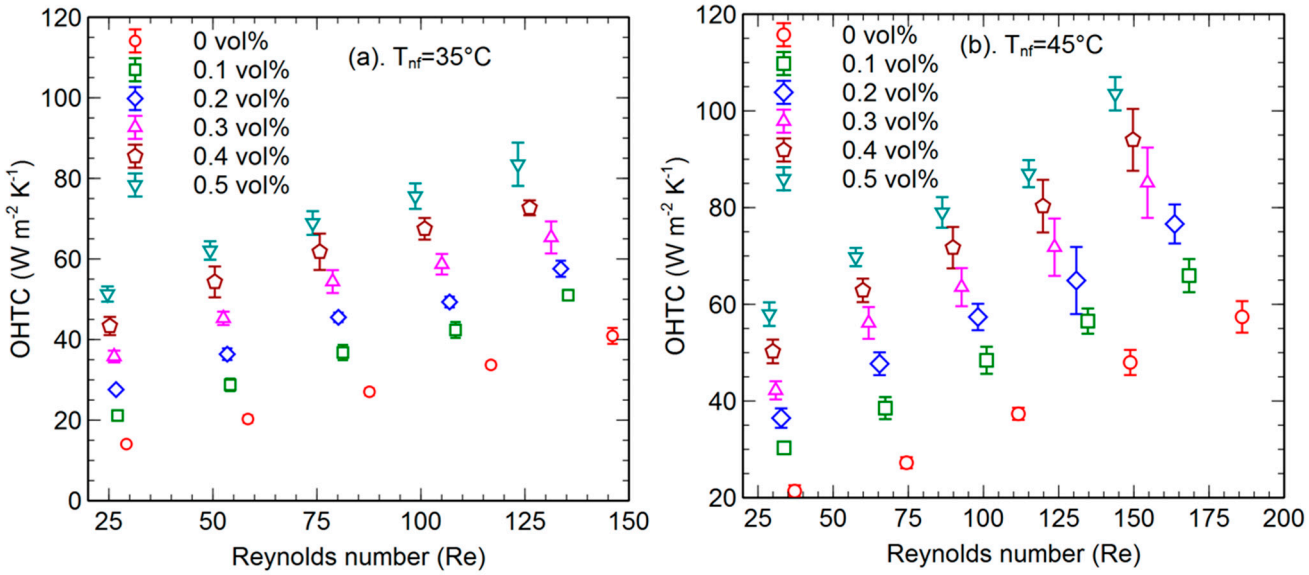

Figure 9. OHTC with respect to Re for various GnP loadings at 5 m/s [108].

Table 11. Summary of published literature on Convective Heat Transfer Characteristics of Graphene-based Nanofluids.

S. No.	Author/Year	Base Fluid	Reynolds Number Range	Test Section	Specification	Enhancement at Higher Concentration (%)	Mechanism	ΔP at Higher Concentration (kPa)
1	Baby et al. (2011) [30]	DI water, EG	15,500 1000	Straight stainless steel tube	Heated by copper wire	171% at 0.01% 219% at 0.01%	Brownian motion, restacking of nanoplatelets, surface area, shape, and size effect	-
2	Ghozatloo et al. (2013) [34]	Ethylene glycol	2840	Straight pipe	Constant heat flux	42.4% at 0.15%	Increase in k	-
3	Amiri et al. (2015) [37]	EG/water (40/60)	-	Car radiator	-	130% at 0.0955%	Decrement in δ_t	0.55
4	Arzani et al. (2015) [38]	DI water	17,000	Annular tube	-	22% at 0.045%	High k of base fluid with GnP, Brownian motion	2.250
5	Mehrali et al. (2016) [40]	DI water	-	-	-	27% at 4%	Increment in k and decrement in δ_t	0.62
6	Yarmand et al. (2016) [41]	DI water	17,500	Stainless steel square pipe	1.4 m length, 10 mm inner width, 12.8 mm outer width	19.68% at 0.045%	Specific surface area, Brownian motion, decrease in δ_t and increase in k of base fluid due to loading of nanoparticles	-
7	Agromayor et al. (2016) [42]	DI water	-	Stainless steel tube in tube heat exchanger	1180 mm length, 10 mmOD, 8 mmID	32% at 0.5%	Increase in k	28
8	Solangi et al. (2016) [43]	Propylene glycol treated water	11,770	Straight seamless copper tube	1500 mm length, 8 mm OD, 4 mm ID	119% at 0.1%	Brownian motion of the nanoparticles, thermal diffusion and thermophoresis, delay and disturbance of the thermal boundary layers, and the excellent k enhancement of the base fluid with nanoparticles	-
9	Amiri et al. (2017) [46]	Transformer oil	-	-	-	32% at 0.0041%	Increment in k of base fluid with GnP and decrement in δ_t	-
10	Ghozatloo et al. (2014) [57]	DI water	1940	Horizontal circular copper tube	1 m length, 1.07 cm ID, 1.30 cm OD	23.9% at 0.045%	Brownian motion, increase in k of nanofluids, decrease in δ_t	-
11	Sadaghinezhad et al. (2014) [64]	DI water	-	Straight stainless steel tube	1400 mm length, 12 mm OD, 10 mm ID	160% at 0.0454%	Delay and disturbance of the thermal boundary layers and excellent k enhancement of the GnP nanofluids, Brownian motion	3.6
12	Zanjani et al. (2014) [65]	DI water	10,850	Uniformly heated copper tube	2740.2 mm length, 4.2 mm ID, 6 mm OD	6.04% at 0.02%	Enhanced effective k of the working fluid resulted from addition of nanoplatelets into the flow field, frequent collision between the nanosheets, base fluid, and the tube wall. Existing fluctuations in the turbulent flow regime, high specific surface area of nanosheets	62.2

Table 11. *Cont.*

S. No.	Author/Year	Base Fluid	Reynolds Number Range	Test Section	Specification	Enhancement at Higher Concentration (%)	Mechanism	ΔP at Higher Concentration (kPa)
13	Sadaghinezhad et al. (2015) [67]	DI water	18,187	Straight stainless steel tube	1400 mm length, 12 mmOD, 10 mmID	Nu enhances by 83% at 0.045%	Delay and disturbance of thermal boundary layers and excellent k enhancement of the GnP nanofluids, Brownian motion, and the migration of GnP nanoplatelets	3.6
14	Mehrali et al. (2015) [70]	DI water	-	Straight stainless steel tube	1400 mm length, 12 mmOD, 10 mmID	200% at 0.045%	Thin boundary layer, improved k, Brownian motion, and specific surface area	-
15	Mehrali et al. (2015) [71]	DI water	-	Straight stainless steel tube	2000 mm, 6.5 mmOD, 4.5 mm ID	15% at 0.045%	Agglomeration of nanoplatelets, Brownian motion of the nanoplatelets, thermal diffusion and Thermophoresis	1.17
16	Kim et al. (2016) [78]	DI water	-	Heat pipe	-	25% at 0.03%	-	-
17	Naghash et al. (2016) [80]	DI water	6000	Straight copper tube	109 cm length, 11 mmID	34% at 0.1%	Increment in k of nanofluids	-
18	Zanjani et al. (2016) [83]	DI water	1760	Uniformly heated copper tube	2740.2 mm length, 4.2 mmID, 6 mmOD	14% at 0.045%	-	-
19	Agarwalet al. (2016) [90]	Kerosene	25,000	Long stainless steel tube	12 m long, 9.5 mmOD, 0.9 mm thick	45% at 0.09%	Increament in k, particle re-arrangement; shear induced thermal conduction enhancement and reduction in δ_t due to agglomeration and clustered structure, at higher concentration	-
20	Goodarzi et al. (2016) [91]	DI water	15,000	Double pipe heat exchanger	-	15.86% at 0.06%	Brownian motion effect on nanoplatelets, Increase in overall k, Increase in effective heat transfer surface area between suspended nanosheets and base fluid	-
21	Ranjbarzadeh et al. (2017) [93]	DI water	-	Copper tube	8.5 mm ID 10 mm OD	40.3% at 0.1%	Flow turbulences at higher Reynolds number and the desired high-potential thermal properties of nanofluid	6.4
22	Arshad et al. (2017) [103]	DI water	-	Micro channel heat sink	-	21.51%	More stability of nanoparticles at lower heat flux	-
23	Selvam et al. (2017) [105]	EG/Water (30/70)	6790	Tube in tube heat exchanger	2.97 m, 10.5 mmOD, 4.3 mmID	170% at 0.5%	Improved thermal conductivity and thermal diffusivity of dispersion, particle clustering, and reduction of δ_t, the high aspect ratio and high k of nanoparticles that participate in the energy transfer process between the fluid and the tube wall	59.13

Table 11. *Cont.*

S. No.	Author/Year	Base Fluid	Reynolds Number Range	Test Section	Specification	Enhancement at Higher Concentration (%)	Mechanism	ΔP at Higher Concentration (kPa)
24	Selvam et al. (2017) [107]	EG/Water (30/70)	250	Automobile radiator	340 mm × 300 mm	80% enhancement at 0.5%	Improved k of nanofluids, particle clustering, particle migration and reduction of δ_t	4.75
25	Selvam et al. (2017) [108]	EG/Water (30/70)	150	Automobile radiator	340 mm × 300 mm	125% enhancement at 0.5%	Improved k of nanofluids, particle clustering, particle migration, and reduction δ_t	7.2 Enhances by 32%
26	Vishnuprasad et al. (2017) [110]	DI water	650	Aluminium metal block	40 mm × 40 mm × 20 mm	78.5% enhancement at 0.2vol%	Enhanced k due to the addition of GnP	Enhances less than 5%
27	Balaji et al. (2020) [113]	DI water	1700	Copper microchannel heat sink	30 mm × 30 mm × 5 mm	71% enhancement at 0.2vol%	Enhanced k due to the addition of GnP	Enhances less than 5%

5. Conclusions

This article has presented a critical overview of the preparation and heat transport characteristics of graphene-based nanofluids from the published literature. Various methods adopted for the preparation of graphene-based nanofluids and its stability characterization have also been explored. However, the graphene-based nano-dispersion shows a better stability due to its excellent properties. However, there is a lack of experimental evidence on the long-term stability of prepared nano-dispersions. Hence, more studies are needed for the exact prediction of the long-term stability of graphene-based nano-dispersions.

From the published literature, it is evident that the enhancement in thermal conductivity of graphene-based nanofluids promotes its usage for improving the heat transport characteristics in various fields of application. Some limitations in the measurement techniques and lack of understanding among the mechanisms are seen as responsible for the enhancement in thermal conductivity. There are many controversial views between the researchers on the mechanisms behind the enhancement in thermal conductivity of graphene-based nano-dispersions. Hence, further research work is needed for prediction of enhancement in thermal conductivity with respect to particle concentration and temperature.

A review of the convective heat transfer coefficients of graphene-based nanofluids shows increase in the heat transfer coefficient with increase in particle volume concentration for a fixed Reynolds number. The higher thermal conductivity and high aspect ratio of graphene nanoplatelets resulted in greater enhancement in thermal conductivity which, in turn, resulted in a higher heat transfer coefficient. The mechanisms behind the enhancement in convective heat transfer coefficient have been analyzed and reported. Many contradictory mechanisms have been seen as the cause for enhancement in convective heat transfer coefficient reported by researchers. Hence, more experimental evidence is needed for prediction of the mechanisms that cause the enhancement in convective heat transfer coefficient. Further research works can help improvement in the heat transfer characteristics of graphene-based nanofluids with the addition of some other materials which make significant improvement in the heat transport properties.

6. Scope for Future Work

The present study deals with the preparation, stability, thermophysical properties, heat transfer behavior, and potential industrial applications of graphene nanofluids. There are still some possible areas that need to be studied. There is a further need to improve the design and the performance of thermal systems despite the higher heat transfer rate of graphene nanofluids. There is yet to be a possible solution to overcome the agglomeration and sedimentation of nanofluids which slows down the interest of the industrial community in commercializing the nanofluids. Further research must enhance nanofluids' thermal

and chemical stability based on optimum and compatible amounts of various surfactant and surface modification techniques. Different graphene nanomaterials' size and shape effect requires further investigation, which overcomes the production challenges of the nanofluids. Limited studies are available on the compatibility of graphene nanofluids with other materials to study the corrosion phenomenon in various high-temperature thermal applications. Hence research needs to investigate the heat transfer performance of graphene nanofluids for the thermal management of high-heat flux electronic devices, batteries, fuel cells, and solar thermal energy harvesting systems. Theoretical models to explain the empirical data have to be developed based on various parameters that affect the heat transfer performance of graphene-based nanofluids. Graphene utilization in Nanomedical applications has significant scope. Further research needs methods for synthesizing graphene, which promotes easier graphene production with ideal properties. The phase change heat transfer, such as condensation and boiling heat transfer, latent heat of condensation and vaporization, and relevant thermodynamics parameters at low and high temperatures are further areas suggested for study.

Author Contributions: Conceptualization, T.B. and C.S.; methodology, T.B. and C.S.; investigation, D.M.L. and C.S.; writing—original draft preparation, T.B. and C.S.; writing—review and editing, T.B. and C.S.; visualization, D.M.L.; supervision, D.M.L.; project administration, D.M.L.; funding acquisition, T.B. All authors have read and agreed to the published version of the manuscript.

Funding: This research was funded by DST INSPIRE- IF 170570.

Conflicts of Interest: The authors declare no conflict of interest.

Nomenclature

GnP	Graphene nano Platelets
DI	Deionized Water
EG	Ethylene Glycol
H_2O	Water
SDBS	Sodium Dodecly Benzene Sulphonate
SDS	Sodium Dodecyl Sulphonate
CMC	Carboxy Methyl Cellulose
PVA	Poly Vinyl Alcohol
CTAB	Cetyl Trimethyl Ammonium Bromide
GA	Gum Arabic
SDC	Sodium Deoxy Cholate
CNT	Carbon Nano Tubes
DEM	Differential Effective Medium
RGO	Reduced Graphene Oxide
GO	Graphene Oxide
CHTC	Convective Heat Transfer Coefficient
OHTC	Overall Heat Transfer Coefficient
SEM	Scanning Electron Microscope
TEM	Transmission Electron Microscope
DLS	Dynamic Light Scattering
UV Vis	Ultra Violet Visible Spectroscopy
XRD	X-Ray Diffraction
FTIR	Fourier Transform Infra Red spectroscopy
AFM	Atomic Force Microscopy
SEM	Field Emission Scanning Electron Microscopy
XPS	X-Ray Photoelectron Spectroscopy
EDS	Energy Dispersive X-Ray Spectroscopy
ESEM	Environmental Scanning Electron Microscopy
BET	Brunauer Emmett Teller
SAED	Selected Area Electron Diffraction
STEM	Scanning Transmission Electron Microscopy

Greek symbols	
k	thermal conductivity of nanofluids
δ_t	thermal boundary layer thickness
ρ	density of nanofluids
C_p	Specific heat of nanofluids
μ	dynamic viscosity of nanofluids
h	heat transfer coefficient

References

1. Younes, H.; Christensen, G.; Luan, X.; Hong, H.; Smith, P. Effects of alignmnet, ph, surfactant, and solvent on heta transfer nanofluids conataining Fe_2O_3 and CuO nanoaprticles. *J. Appl. Phys.* **2012**, *111*, 064308. [CrossRef]
2. Christensen, G.; Younes, H.; Hong, H.; Smith, P. Effects of solvent hydrogen bonding, viscosity, and polarity on the dispersion and alignment of nanofluids containing Fe_2O_3 nanoparticles. *J. Appl. Phys.* **2015**, *118*, 214302. [CrossRef]
3. Christensen, G.; Younes, H.; Hong, H.; Peterson, G.P. Alignment of carbon nanotubes comprising magnetically sensitive metal oxides by non–ionic chemical surfactants. *J. Nanofluids* **2013**, *2*, 25–28. [CrossRef]
4. Choi, S.U.; Eastman, J.A. *Enhancing Thermal Conductivity of Fluids with Nanoparticles*; Argonne National Lab.: Argonne, IL, USA, 1995.
5. Rasheed, A.K.; Khalid, M.; Rashmi, W.; Gupta, T.C.; Chan, A. Graphene based nanofluids and nanolubricants–review of recent developments. *Renew. Sustain. Energy Rev.* **2016**, *63*, 346–362. [CrossRef]
6. Wang, X.Q.; Mujumdar, A.S. Heat transfer characteristics of nanofluids: A review. *Int. J. Therm. Sci.* **2007**, *46*, 1–19. [CrossRef]
7. Trisaksri, V.; Wongwises, S. Critical review of heat transfer characteristics of nanofluids. *Renew. Sustain. Energy Rev.* **2007**, *11*, 512–523. [CrossRef]
8. Kakaç, S.; Pramuanjaroenkij, A. Review of convective heat transfer enhancement with nanofluids. *Int. J. Heat Mass Transf.* **2009**, *52*, 3187–3196. [CrossRef]
9. Godson, L.; Raja, B.; Mohan Lal, D.; Wongwises, S. Enhancement of heat transfer using nanofluids-An overview. *Renew. Sustain. Energy Rev.* **2010**, *14*, 629–641. [CrossRef]
10. Saidura, R.; Leong, K.Y.; Mohammad, H.A. A review on applications and challenges of nanofluids. *Renew. Sustain. Energy Rev.* **2011**, *15*, 1646–1668. [CrossRef]
11. Chandrasekar, M.; Suresh, S.; Senthilkumar, T. Mechanisms proposed through experimental investigations on thermophysical properties and forced convective heat transfer characteristics of various nanofluids–A review. *Renew. Sustain. Energy Rev.* **2012**, *16*, 3917–3938. [CrossRef]
12. Alawi, O.A.; Sidik, N.A.; Mohammed, H.A.; Syahrullail, S. Fluid flow and heat transfer characteristics of nanofluids in heat pipes: A review. *Int. Commun. Heat Mass Transf.* **2014**, *56*, 50–62. [CrossRef]
13. Raja, M.; Vijayan, R.; Dineshkumar, P.; Venkatesan, M. Review on nanofluids characterization, heat transfer characteristics and applications. *Renew. Sustain. Energy Rev.* **2016**, *64*, 163–173. [CrossRef]
14. Ganvir, R.B.; Walke, P.V.; Kriplani, V.M. Heat transfer characteristics in nanofluid—A review. *Renew. Sustain. Energy Rev.* **2017**, *75*, 451–460. [CrossRef]
15. Sajid, M.U.; Ali, H.M. Recent advances in application of nanofluids in heat transfer devices: A critical review. *Renew. Sustain. Energy Rev.* **2019**, *103*, 556–592. [CrossRef]
16. Sureshkumar, R.; Mohideen, S.T.; Nethaji, N. Heat transfer characteristics of nanofluids in heat pipes: A review. *Renew. Sustain. Energy Rev.* **2013**, *20*, 397–410. [CrossRef]
17. Pavía, M.; Alajami, K.; Estellé, P.; Desforges, A.; Vigolo, B. A critical review on thermal conductivity enhancement of graphene-based nanofluids. *Adv. Colloid Interface Sci.* **2021**, *294*, 102452. [CrossRef]
18. Amani, M.; Amani, P.; Bahiraei, M.; Ghalambaz, M.; Ahmadi, G.; Wang, L.-P.; Wongwises, S.; Mahian, O. Latest developments in nanofluid flow and heat transfer between parallel surfaces: A critical review. *Adv. Colloid Interface Sci.* **2021**, *294*, 102450. [CrossRef]
19. Angayarkanni, S.A.; Philip, J. Review on thermal properties of nanofluids: Recent developments. *Adv. Colloid Interface Sci.* **2015**, *225*, 146–176. [CrossRef] [PubMed]
20. Philip, J.; Shima, P.D. Thermal properties of nanofluids. *Adv. Colloid. Interface Sci.* **2012**, *183–184*, 30–45. [CrossRef]
21. Keblinski, P.; Eastman, J.A.; Cahill, D.G. Nanofluids for thermal transport. *Mater. Today* **2005**, *8*, 36–44. [CrossRef]
22. Donaldson, L. Diamond nanoparticles improve heat transfer. *Mater. Today* **2014**, *17*, 212. [CrossRef]
23. Koratkar, N.A. *Graphene in Composite Materials: Synthesis, Characterization and Applications*; DEStech Publications, Inc.: Lancaster, PA, USA, 2013.
24. Sadeghinezhad, E.; Mehrali, M.; Saidur, R.; Mehrali, M.; Latibari, S.T.; Akhiani, A.R.; Metselaar, H.S. A comprehensive review on graphene nanofluids: Recent research, development and applications. *Energy Convers. Manag.* **2016**, *111*, 466–487. [CrossRef]
25. Tarelho, J.P.G.; Santos, M.P.S.; Ferreira, J.A.F.; Ramos, A.; Kopyl, S.; Kim, S.O.; Hong, S.; Kholkin, A. Graphene-based materials and structures for energy harvesting with fluids—A review. *Mater. Today* **2018**, *21*, 1019–1041. [CrossRef]
26. Singh, S.B.; De, M. Thermally exfoliated graphene oxide for hydrogen storage. *Mater. Chem. Phys.* **2020**, *239*, 122102. [CrossRef]

27. Singh, S.B.; De, M. Improved hydrogen uptake of metal modified reduced and exfoliated graphene oxide. *J. Mater. Sci. Res.* **2021**, *36*, 3109–3120. [CrossRef]
28. Singh, S.B.; De, M. Effects of gaseous environments on physiochemical properties of thermally exfoliated graphene oxides for hydrogen storage: A comparative study. *J. Porous Mater* **2021**, *28*, 875–888. [CrossRef]
29. Gupta, S.S.; Siva, V.M.; Krishnan, S.; Sreeprasad, T.S.; Singh, P.K.; Pradeep, T.; Das, S.K. Thermal conductivity enhancement of nanofluids containing graphene nanosheets. *J. Appl. Phys.* **2011**, *110*, 084302. [CrossRef]
30. Baby, T.T.; Ramaprabhu, S. Enhanced convective heat transfer using graphene dispersed nanofluids. *Nanoscale Res. Lett.* **2011**, *6*, 289. [CrossRef]
31. Ghozatloo, A.; Shariaty-Niasar, M.; Rashidi, A.M. Preparation of nanofluids from functionalized Graphene by new alkaline method and study on the thermal conductivity and stability. *Int. Commun. Heat Mass Transf.* **2013**, *42*, 89–94. [CrossRef]
32. Maa, W.; Yanga, F.; Shia, J.; Wang, F.; Zhang, Z.; Wang, S. Silicone based nanofluids containing functionalized graphene nanosheets. *Physicochem. Eng. Aspects.* **2013**, *431*, 120–126. [CrossRef]
33. Kole, M.; Dey, T.K. Investigation of thermal conductivity, viscosity, and electrical conductivity of graphene based nanofluids. *J. Appl. Phys.* **2013**, *113*, 084307. [CrossRef]
34. Ghozatloo, M.; Shariaty-Niasar, A.M.; RashidiInt, J. Investigation of Heat Transfer Coefficient of Ethylene Glycol/ Graphene-nanofluid in Turbulent Flow Regime. *Nanosci. Nanotechnol.* **2014**, *10*, 237–244.
35. Farid, S.; Shirazi, S.; Gharehkhani, S.; Yarmand, H.; Badarudin, A.; Metselaar, H.S.C.; Kazi, S.N. Nitrogen doped activated carbon /graphene with high nitrogen level: Green synthesis and thermo-electrical properties of its nanofluid. *Mater. Lett.* **2015**, *152*, 192–195.
36. Amiri, A.; Sadri, R.; Shanbedi, M.; Ahmadi, G.; Chew, B.; Kazi, S.; Dahari, M. Performance dependence of thermosyphon on the functionalization approaches: An experimental study on thermo-physical properties of graphene nanoplatelet-based water nanofluids. *Energy Convers. Manag.* **2015**, *92*, 322–330. [CrossRef]
37. Amiri, A.; Sadri, R.; Shanbedi, M.; Ahmadi, G.; Kazi, S.; Chew, B.; Nashrul, M.; Zubir, M. Synthesis of ethylene glycol-treated Graphene Nanoplatelets with one-pot, microwave-assisted functionalization for use as a high performance engine coolant. *Energy Convers. Manag.* **2015**, *101*, 767–777. [CrossRef]
38. Khajeh Arzani, H.; Amiri, A.; Kazi, S.; Chewa, B.; Badarudin, A. Experimental and numerical investigation of thermophysical properties, heat transfer and pressure drop of covalent and noncovalent functionalized graphene nanoplatelet-based water nanofluids in an annular heat exchanger. *Int. Commun. Heat Mass Transf.* **2015**, *68*, 267–275. [CrossRef]
39. Sarsam, W.S.; Amiri, A.; Kazi, S.; Badarudin, A. Stability and thermophysical properties of non-covalently functionalized graphene nanoplatelets nanofluids. *Energy Convers. Manag.* **2016**, *116*, 101–111. [CrossRef]
40. Mehrali, M.; Sadeghinezhad, E.; Akhiani, A.R.; Tahan Latibari, S.; Talebian, S.; Dolatshahi-Pirouz, A.; Metselaar, H.S.C.; Mehrali, M. An ecofriendly graphene-based nanofluid for heat transfer applications. *J. Clean. Prod.* **2016**, *137*, 555–566. [CrossRef]
41. Yarmand, H.; Gharehkhani, S.; Shirazi, S.F.S.; Amiri, A.; Alehashem, M.S.; Dahari, M.; Kazi, S. Experimental investigation of thermo-physical properties, convective heat transfer and pressure drop of functionalized graphene nanoplatelets aqueous nanofluid in a square heated pipe. *Energy Convers. Manag.* **2016**, *114*, 38–49. [CrossRef]
42. Agromayor, R.; Cabaleiro, D.; Pardinas, A.A.; Vallejo, J.P.; Fernandez-Seara, J.; Lugo, L. Heat Transfer Performance of Functionalized Graphene Nanoplatelet Aqueous Nanofluids. *Mater.* **2016**, *9*, 455. [CrossRef]
43. Solangi, K.; Amiri, A.; Luhur, M.; Ghavimi, S.A.A.; Zubir, M.N.M.; Kazi, S.; Badarudin, A. Experimental investigation of the propylene glycol-treated graphene nanoplatelets for the enhancement of closed conduit turbulent convective heat transfer. *Int. Commun. Heat Mass Transf.* **2016**, *73*, 43–53. [CrossRef]
44. Sadri, R.; Hosseini, M.; Kazi, S.; Bagheri, S.; Zubir, N.; Ahmadi, G.; Dahari, M.; Zaharinie, T. A novel, eco-friendly technique for covalent functionalization of graphene nanoplatelets and the potential of their nanofluids for heat transfer applications. *Chem. Phys. Lett.* **2017**, *675*, 92–97. [CrossRef]
45. Amiri, A.; Shanbedi, M.; Dashti, H. Thermophysical and rheological properties of water-based graphene quantum dots nanofluids. *J. Taiwan Inst Chem Eng.* **2017**, *76*, 132–140. [CrossRef]
46. Amiri, A.; Shanbedi, M.; Ahmadi, G.; Rozali, S. Transformer oils-based graphene quantum dots nanofluid as a new generation of highly conductive and stable coolant. *Int. Commun. Heat Mass Transf.* **2017**, *83*, 40–47. [CrossRef]
47. Esfahani, M.R.; Languri, E.M. Exergy analysis of a shell-and-tube heat exchanger using graphene oxide nanofluids. *Exp. Therm. Fluid Sci.* **2017**, *83*, 100–106. [CrossRef]
48. Jyothirmayee, S.; Ramaprabhu, S. Surfactant free graphene nanosheets based nanaofluids by insitu reduction of graphene oxide suspensions. *J. Appl. Phys.* **2011**, *110*, 124326. [CrossRef]
49. Yu, W.; Xiea, H.; Wang, X.; Wang, X. Significant thermal conductivity enhancement for nanofluids containing graphene nanosheets. *Phys. Lett. A* **2011**, *375*, 1323–1328. [CrossRef]
50. Park, S.; Lee, S.W.; Kang, S.; Kim, S.M.; Bang, I.C. Pool boiling CHF enhancement by graphene-oxide nanofluid under nuclear coolant chemical environments. *Nucl. Eng. Des.* **2012**, *252*, 184–191. [CrossRef]
51. Wanga, B.; Wanga, X.; Loua, W.; Haoa, J. Colloids and Surfaces Thermal conductivity and rheological properties of graphite/oil nanofluids. *Physicochem. Eng. Asp.* **2012**, *414*, 125–131. [CrossRef]
52. Ahn, S.H.; Kim, J.M.; Kim, M.H. Experimental study of the effect of a reduced graphene oxide coating on critical heat flux enhancement. *Int. J. Heat Mass Transf.* **2013**, *60*, 763–771. [CrossRef]

53. Li, B.; Liu, T.; Hua, L.; Wang, Y.; Nie, S. Facile preparation and adjustable thermal property of stearic acid–graphene oxide composite as shape-stabilized phase change material. *J. Chem. Eng.* **2013**, *215–216*, 819–826. [CrossRef]
54. Park, S. In Cheol Bang. Flow boiling CHF enhancement in an external reactor vessel cooling(ERVC) channel using graphene oxide nanofluid. *Nucl. Eng. Des.* **2013**, *265*, 310–318. [CrossRef]
55. Moghaddam, M.B.; Goharshadi, E.K.; Entezari, M.H.; Nancarrow, P. Preparation, characterization, and rheological properties of graphene–glycerol nanofluids. *J. Chem. Eng.* **2013**, *231*, 365–372. [CrossRef]
56. Lee, S.W.; Kim, K.M. In Cheol Bang. Study on flow boiling critical heat flux enhancement of graphene oxide/water nanofluid. *Int. J. Heat Mass Transf.* **2013**, *65*, 348–356. [CrossRef]
57. Ghozatloo, A.; Rashidi, A.; Shariaty-Niassar, M. Convective heat transfer enhancement of graphene nanofluids in shell and tube heat exchanger. *Exp. Therm. Fluid Sci.* **2014**, *53*, 136–141. [CrossRef]
58. Kim, J.M.; Kim, T.; Kim, J.; Kim, M.H.; Ahn, H.S. Effect of a graphene oxide coating layer on critical heat flux enhancement under pool boiling. *Int. J. Heat Mass Transf.* **2014**, *77*, 919–927. [CrossRef]
59. Jiaa, L.; Chena, Y.; Leia, S.; Moa, S.; Liua, Z.; Shaoa, X. Effect of magnetic field and surfactant on dispersion of Graphene/water nanofluid during solidification. *Energy Procedia* **2014**, *61*, 1348–1351. [CrossRef]
60. Zhang, L.; Pu, J.; Wang, L.; Xue, Q. Frictional dependence of graphene and carbon nanotube in diamond-like carbon/ionic liquids hybrid films in vacuum. *Carbon* **2014**, *80*, 734–745. [CrossRef]
61. Ahn, H.S.; Kim, J.M.; Kaviany, M.; Kim, M.H. Pool boiling experiments in reduced graphene oxide colloids. *Int. J. Heat Mass Transf.* **2014**, *74*, 501–512. [CrossRef]
62. Liu, J.; Wang, F.; Zhang, L.; Fang, X.; Zhang, Z. Thermodynamic properties and thermal stability of ionic liquid-based nanofluids containing graphene as advanced heat transfer fluids for medium-to-high-temperature applications. *Renew. Energ.* **2014**, *63*, 519–523. [CrossRef]
63. Li, X.; Chen, Y.; Cheng, Z.; Jia, L.; Mo, S.; Liu, Z. Ultrahigh specific surface area of graphene for eliminating subcooling of water. *Appl. Energy.* **2014**, *130*, 824–829. [CrossRef]
64. Sadeghinezhad, E.; Mehrali, M.; TahanLatibari, S.; Mehrali, M.; Oon, C.S.; Metselaar, H.S.C. Experimental Investigation of Convective Heat Transfer Using Graphene Nanoplatelet Based Nanofluids under Turbulent Flow Conditions. *Ind. Eng. Chem. Res.* **2014**, *53*, 12455–12465. [CrossRef]
65. Akhavan-Zanjani, H.; Saffar-Avval, M.; Mansourkiaei, M.; Ahadi, M.; Sharif, F. Turbulent forced Convective Heat Transfer and Pressure Drop of Graphene–Water Nanofluid Flowing Inside a Horizontal Circular Tube. *J. Dispers. Sci. Technol.* **2014**, *35*, 1532–2351. [CrossRef]
66. Liu, J.; Ye, Z.; Zhang, L.; Fang, X.; Zhang, Z. A combined numerical and experimental study on graphene/ionic liquid nanofluid based direct absorption solar collector. *Sol. Energy Mater. Sol. Cells* **2015**, *136*, 177–186. [CrossRef]
67. Sadeghinezhad, E.; Togun, H.; Mehrali, M.; Nejad, P.S.; Latibari, S.T.; Abdulrazzaq, T.; Kazi, S.; Metselaar, H.S.C. An experimental and numerical investigation of heat transfer enhancement for graphene nanoplatelets nanofluids in turbulent flow conditions. *Int. J. Heat Mass Transf.* **2015**, *81*, 41–51. [CrossRef]
68. Yudong, L.; Chuangjian, S.; Pengfei, H.; Quangui, P.; Liuzhu, W.; Jiangqing, W. Containerless nucleation behavior and supercooling degree of acoustically levitated graphene oxide nanofluid PCM. *Int. J. Refrig.* **2015**, *60*, 70–80. [CrossRef]
69. Leia, S.; Chena, Y.; Jiaa, L. Directional Solidification of Graphene/Paraffin nanofluids assisted by electromagnetic field. *Energy Procedia* **2015**, *75*, 3290–3294. [CrossRef]
70. Mehrali, M.; Sadeghinezhad, E.; Rosen, M.A.; Latibari, T.S.; Mehrali, M.; Metselaar, H.S.C.; Newaz Kazi, S. Effect of specific surface area on convective heat transfer of graphene nanoplatelet aqueous nanofluids. *Exp. Therm. Fluid Sci.* **2015**, *68*, 100–108. [CrossRef]
71. Mehrali, M.; Sadeghinezhad, E.; Rosen, M.A.; Akhiani, A.R.; Tahan Latibari, S.; Mehrali, M.; Metselaar, H.S.C. Heat transfer and entropy generation for laminar forced convection flow of graphene nanoplatelets nanofluids in a horizontal tube. *Int. Commun. Heat Mass Transf.* **2015**, *66*, 23–31. [CrossRef]
72. Ijam, A.; Saidur, R.; Ganesan, P.; Golsheikh, A.M. Stability, thermo-physical properties, and electrical conductivity of graphene oxide-Deionized water/ethylene glycol based nanofluid. *Int. Commun. Heat Mass Transf.* **2015**, *87*, 92–103. [CrossRef]
73. Liu, Y.; Li, X.; Hu, P.; Hu, G. Study on the supercooling degree and nucleation behavior of water-based graphene oxide nanofluids PCM. *Int. J. Refrig.* **2015**, *50*, 80–86. [CrossRef]
74. Kamatchi, R.; Venkatachalapathy, S.; Srinivas, B.A. Synthesis, stability, transport properties, and surface wettability of reduced graphene oxide/water nanofluids. *Int. J. Therm. Sci.* **2015**, *97*, 17–25. [CrossRef]
75. Fan, L.-W.; Li, J.-Q.; Li, D.-Y.; Zhang, L.; Yu, Z.-T.; Cen, K.-F. The effect of concentration on transient pool boiling heat transfer of graphene-based aqueous nanofluids. *Int. J. Therm. Sci.* **2015**, *91*, 83–95. [CrossRef]
76. Askari, S.; Lotfi, R.; Seifkordi, A.; Rashidi, A.; Koolivand, H. A novel approach for energy and water conservation in wet cooling towers by using MWNTs and nanoporous graphene nanofluids. *Energy Convers. Manag.* **2016**, *109*, 10–18. [CrossRef]
77. Esfahani, M.R.; Mohseni Languri, E.; Nunna, M.R. Effect of particle size and viscosity on thermal conductivity enhancement of graphene oxide nanofluid. *Int. Commun. Heat Mass Transf.* **2016**, *76*, 308–315. [CrossRef]
78. Kim, K.M. In Cheol Bang. Effects of graphene oxide nanofluids on heat pipe performance and capillary limits. *Int. J. Therm. Sci.* **2016**, *100*, 346–356.

79. Iranmanesh, S.; Mehrali, M.; Sadeghinezhad, E.; Ang, B.C.; Ong, H.; Esmaeilzadeh, A. Evaluation of viscosity and thermal conductivity of graphene nanoplatelets nanofluids through a combined experimental –statistical approach using respond surface methodology method. *Int. Commun. Heat Mass Transf.* **2016**, *79*, 74–80. [CrossRef]
80. Naghash, A.; Sattari, S.; Rashidi, A. Experimental assessment of convective heat transfer coefficient enhancement of nanofluids prepared from high surface area nanoporous graphene. *Int. Commun. Heat Mass Transf.* **2016**, *78*, 127–134. [CrossRef]
81. Tahani, M.; Vakili, M.; Khosrojerdi, S. Experimental evaluation and ANN modeling of thermal conductivity of graphene oxide nanoplatelets/Deionized water nanofluid. *Int. Commun. Heat Mass Transf.* **2016**, *76*, 358–365. [CrossRef]
82. Vakili, M.; Hosseinalipour, S.; Delfani, S.; Khosrojerdi, S.; Karami, M. Experimental investigation of graphene nanoplatelets nanofluid-based volumetric solar collector for domestic hot water systems. *Sol. Energy* **2016**, *131*, 119–130. [CrossRef]
83. Akhavan-Zanjani, H.; Saffar-Avval, M.; Mansourkiaei, M.; Sharif, F.; Ahadi, M. Experimental investigation of laminar forced convective heat transfer of Graphenee water nanofluid inside a circular tube. *Int. J. Therm. Sci.* **2016**, *100*, 316–323. [CrossRef]
84. Jiaa, L.; Chen, Y.; Lei, S.; Mo, S.; Luo, X.; Shao, X. External electromagnetic field-aided freezing of CMC-modified graphene/water nanofluid. *Appl. Energy* **2016**, *162*, 1670–1677. [CrossRef]
85. Vakili, M.; Hosseinalipour, S.; Delfani, S.; Khosrojerdi, S. Photothermal properties of graphene nanoplatelets nanofluid for low-temperature direct absorption solar collectors. *Sol. Energy Mater. Sol. Cells* **2016**, *152*, 187–191. [CrossRef]
86. Sarsama, W.S.; Amiri, A.; Mohd Zubira, M.; Yarmanda, H.; Kazi, S.; Badarudinaa, A. Stability and thermophysical properties of water-based nanofluids containing triethanolamine-treated graphene nanoplatelets with different specific surface areas. *Physicochem. Eng. Asp.* **2016**, *500*, 17–31. [CrossRef]
87. Tharayil, T.; Asirvatham, L.G.; Ravindran, V.; Wongwises, S. Thermal performance of miniature loop heat pipe with graphene–water nanofluid. *Int. J. Heat Mass Transf.* **2016**, *93*, 957–968. [CrossRef]
88. Khosrojerdi, S.; Vakili, M.; Yahyaei, M.; Kalhor, K. Thermal conductivity modeling of graphene nanoplatelets/Deionized water nanofluid by MLP neural network and theoretical modeling using experimental results. *Int. Commun. Heat Mass Transf.* **2016**, *74*, 11–17. [CrossRef]
89. Ahammed, N.; Asirvathama, L.G.; Titus, J.; Bose, J.R.; Wongwises, S. Measurement of thermal conductivity of graphene–water nanofluid at below and above ambient temperatures. *Int. Commun. Heat Mass Transf.* **2016**, *70*, 66–74. [CrossRef]
90. Agarwal, D.K.; Vaidyanathan, A.; Kumar, S.S. Experimental investigation on thermal performance of kerosene–graphene nanofluid. *Exp. Therm. Fluid Sci.* **2016**, *71*, 126–137. [CrossRef]
91. Goodarzi, M.; Kherbeet, A.; Afrand, M.; Sadeghinezhadd, E.; Mehrali, M.; Zahedi, P.; Wongwises, S.; Dahari, M. Investigation of heat transfer performance and friction factor of a counter-flow double-pipe heat exchanger using nitrogen-doped, graphene-based nanofluids. *Int. Commun. Heat Mass Transf.* **2016**, *76*, 16–23. [CrossRef]
92. Vakili, M.; Khosrojerdi, S.; Aghajannezhad, P.; Yahyaei, M. A hybrid artificial neural network-genetic algorithm modeling approach for viscosity estimation of graphene nanoplatelets nanofluid using experimental data. *Int. Commun. Heat Mass Transf.* **2017**, *82*, 40–48. [CrossRef]
93. Ranjbarzadeh, R.; Karimipour, A.; Afrand, M.; Homayoon, A.; Isfahani, M.; Shirneshan, A. Empirical analysis of heat transfer and friction factor of water/graphene oxide nanofluid flow in turbulent regime through an isothermal pipe. *Appl. Therm. Eng.* **2017**, *126*, 538–547. [CrossRef]
94. Tharayil, T.; Asirvatham, L.G.; Dau, M.J.; Wongwises, S. Entropy generation analysis of a miniature loop heat pipe with graphene–water nanofluid: Thermodynamics model and experimental study. *Int. J. Heat Mass Transf.* **2017**, *106*, 407–421. [CrossRef]
95. Khosrojerdia, S.; Lavasani, A.M.; Vakilic, M. Experimental study of photothermal specifications and stability of graphene oxide nanoplatelets nanofluid as working fluid for low-temperature Direct Absorption Solar Collectors (DASCs). *Sol. Energy Mater. Sol. Cells* **2017**, *164*, 32–39. [CrossRef]
96. Zang, C.; Zhang, L.; Xu, H.; Wang, D.; Ye, B. Investigation of flow boiling performance and the resulting surface deposition of graphene oxide nanofluid in microchannels. *Exp. Therm. Fluid Sci.* **2017**, *86*, 1–10. [CrossRef]
97. Liu, Y.; Wang, J.; Su, C.; Geng, S.; Gao, Y.; Peng, Q. Nucleation rate and supercooling degree of water-based graphene oxide nanofluids. *Appl. Therm. Eng.* **2017**, *115*, 1226–1236.
98. Chen, L.; Xu, C.; Liu, J.; Fang, X.; Zhang, Z. Optical absorption property and photo-thermal conversion performance of graphene oxide/water nanofluids with excellent dispersion stability. *Sol. Energy* **2017**, *148*, 17–24. [CrossRef]
99. Iranmanesh, S.; Ong, H.C.; Ang, B.C.; Sadeghinezhad, E.; Esmaeilzadeh, A.; Mehrali, M. Thermal performance enhancement of an evacuated tube solar collector using graphene nanoplatelets nanofluid. *J. Clean. Prod.* **2017**, *162*, 121–129. [CrossRef]
100. Wang, N.; Xu, G.; Li, S.; Zhang, X. Thermal Properties and Solar Collection Characteristics of Oil-based Nanofluids with Low Graphene Concentration. In Proceedings of the 8th International Conference on Applied Energy–ICAE, Beijing, China, 8–11 October 2016.
101. Chai, Y.H.; Yusup, S.; Chok, V.S.; Irawan, S.; Singh, J.S.D.B. Thermophysical properties of graphene nanosheets–Hydrogenated oil based nanofluid for drilling fluid improvements. *Appl. Therm. Eng.* **2017**, *122*, 794–805. [CrossRef]
102. Ali, H.M.; Arshad, W. Effect of channel angle of pin-fin heat sink on heat transfer performance using water based graphene nanoplatelets nanofluids. *Int. J. Heat Mass Transf.* **2017**, *106*, 465–472. [CrossRef]
103. Arshad, W.; Ali, H.M. Graphene nanoplatelets nanofluids thermal and hydrodynamic performance on integral fin heat sink. *Int. J. Heat Mass Transf.* **2017**, *107*, 995–1001. [CrossRef]

104. Selvam, C.; Lal, D.M.; Harish, S. Thermal conductivity enhancement of ethylene glycol and water with graphene nanoplatelets. *Thermochim. Acta* **2016**, *642*, 32–38. [CrossRef]
105. Selvam, C.; Balaji, T.; Lal, D.M.; Harish, S. Convective heat transfer coefficient and pressure drop of water-ethylene glycol mixture with graphene nanoplatelets. *Exp. Therm. Fluid Sci.* **2017**, *80*, 67–76. [CrossRef]
106. Selvam, C.; Lal, D.M.; Harish, S. Thermal conductivity and specific heat capacity of water-ethylene glycol mixture-based nanofluids with graphene nanoplatelets. *J. Therm. Anal. Calorim.* **2017**, *129*, 947–955. [CrossRef]
107. Selvam, C.; Lal, D.M.; Harish, S. Enhanced heat transfer performance of an automobile radiator with graphene based suspensions. *Appl. Therm. Eng.* **2017**, *123*, 50–60. [CrossRef]
108. Selvam, C.; Raja, R.S.; Lal, D.M.; Harish, S. Overall heat transfer coefficient improvement of an automobile radiator with graphene based suspensions. *Int. J. Heat Mass Transf.* **2017**, *115*, 580–588. [CrossRef]
109. Sidney, S.; Lal, D.M.; Selvam, C.; Harish, S. Experimental Investigation of Freezing and Melting Characteristics of Graphene-Based Phase Change Nanocomposite for Cold Thermal Energy Storage Applications. *Appl. Sci.* **2019**, *9*, 1099. [CrossRef]
110. Vishnuprasad, S.; Haribabu, K.; Perarasu, V. Experimental study on the convective heat transfer performance and pressure drop of functionalized graphene nanofluids in electronics cooling system. *Heat Mass Transf.* **2019**, *55*, 2221–2234.
111. Saeed, E.; Piñeiro, M.M.; Hermida-Merino, C.; Pastoriza-Gallego, M.J. Determination of Transport Properties of Glycol-Based NanoFluids Derived from Surface Functionalized Graphene. *J. Nanomater.* **2019**, *9*, 252. [CrossRef]
112. Das, S.; Giri, A.; Samanta, S.; Kanagaraj, S. Role of graphene nanofluids on heat transfer enhancement in thermosyphon. *J. Sci.-Ad. Mater. Dev.* **2019**, *4*, 163–169. [CrossRef]
113. Balaji, T.; Selvam, C.; Lal, D.M.; Harish, S. Enhanced heat transport behaviour of micro channel heat sink with graphene based nanofluids. *Int. Commun. Heat Mass Transf.* **2020**, *117*, 104716. [CrossRef]
114. Balandin, A.; Ghosh, S.; Bao, W.; Calizo, I.; Teweldebrhan, D.; Miao, F.; Lau, C. Superior thermal conductivity of single-layer graphene. *Nano Lett.* **2008**, *8*, 902–907. [CrossRef]
115. Ghosh, S.; Calizo, I.; Teweldebrhan, D.; Pokatilov, E.; Nika, D.; Balandin, A.; Bao, W.; Miao, F.; Lau, C. Extremely high thermal conductivity of graphene: Prospects for thermal management applications in nanoelectronic circuits. *Appl. Phys. Lett.* **2008**, *92*, 151911. [CrossRef]
116. Cai, W.; Moore, A.; Zhu, Y.; Li, X.; Chen, S.; Shi, L.; Ruoff, R. Thermal transport in suspended and supported monolayer graphene grown by chemical vapor deposition. *Nano Lett.* **2010**, *10*, 1645–1651. [CrossRef]
117. Jauregui, L.; Yue, Y.; Sidorov, A.; Hu, J.; Yu, Q.; Lopez, G.; Jalilian, R.; Benjamin, D.K.; Delk, D.A.; Wu, W.; et al. Thermal transport in graphene nanostructures: Experiments and simulations. *ECS Trans.* **2010**, *28*, 73–83. [CrossRef]
118. Faugeras, C.; Faugeras, B.; Orlita, M.; Potemski, M.; Nair, R.; Geim, A. Thermal conductivity of graphene in corbino membrane geometry. *ACS Nano* **2010**, *4*, 1889–1892. [CrossRef]
119. Chen, S.S.; Moore, A.; Cai, W.W.; Suk, J.W.; An, J.; Mishra, C.; Amos, C.; Magnuson, C.W.; Kang, J.; Shi, L.; et al. Raman measurements of thermal transport in suspended monolayer graphene of variable sizes in vacuum and gaseous environments. *ACS Nano* **2011**, *5*, 321–328. [CrossRef] [PubMed]
120. Lee, J.-U.; Yoon, D.; Kim, H.; Lee, S.W.; Cheong, H. Thermal conductivity of suspended pristine graphene measured by Raman spectroscopy. *Phys. Rev. B* **2011**, *83*, 081419. [CrossRef]
121. Yu, Y.-J.; Han, M.Y.; Berciaud, S.; Georgescu, A.B.; Heinz, T.F.; Brus, L.E.; Kim, K.S.; Kim, P. High-resolution spatial mapping of the temperature distribution of a Joule self-heated graphene nanoribbon. *Appl. Phys. Lett.* **2011**, *99*, 183105. [CrossRef]
122. Pumarol, M.E.; Rosamond, M.C.; Tovee, P.; Petty, M.C.; Zeze, D.A.; Falko, V.; Kolosov, O.V. Direct nanoscale imaging of ballistic and diffusive thermal transport in graphene nanostructures. *Nano Lett.* **2012**, *12*, 2906–2911. [CrossRef]
123. Yoon, K.; Hwangb, G.; Chungb, J.; Kim, H.; Kwon, O.; Kihm, K.D.; Lee, J.S. Measuring the thermal conductivity of residue-free suspended graphene bridge using null point scanning thermal microscopy. *Carbon* **2014**, *76*, 77–78. [CrossRef]
124. Dorgan, V.E.; Behnam, A.; Conley, H.J.; Bolotin, K.I.; Pop, E. High-field electrical and thermal transport in suspended graphene. *Nano Lett.* **2013**, *13*, 4581–4586. [CrossRef] [PubMed]
125. Bae, M.-H.; Li, Z.; Aksamija, Z.; Martin, P.N.; Xiong, F.; Ong, Z.-Y.; Knezevic, I.; Pop, E. Ballistic to diffusive crossover of heat flow in graphene ribbons. *Nat. Commun.* **2013**, *4*, 1734. [CrossRef]
126. Xu, X.; Pereira, L.F.; Wang, Y.; Wu, J.; Kaiwen, Z.; Zhao, X.; Bae, S.; Bui, C.T.; Xie, R.; Thong, J.T.; et al. Lengthdependent thermal conductivity in suspended single-layer graphene. *Nat. Commun.* **2014**, *5*, 3689. [CrossRef] [PubMed]
127. Seol, J.H.; Moore, A.L.; Shi, L.; Jo, I.; Yao, Z. Thermal conductivity measurement of graphene exfoliated on silicon dioxide. *J. Heat Transfer* **2011**, *133*, 022403-1. [CrossRef]
128. Nika, D.L.; Ghosh, S.; Pokatilov, E.; Balandin, A. Lattice thermal conductivity of graphene flakes: Comparison with bulk graphite. *Appl. Phys. Lett.* **2009**, *94*, 203103. [CrossRef]
129. Munoz, E.; Lu, J.; Yakobson, B.I. Ballistic thermal conductance of graphene ribbons. *Nano Lett.* **2010**, *10*, 1652–1656. [CrossRef] [PubMed]
130. Wei, Z.; Ni, Z.; Bi, K.; Chen, M.; Chen, Y. In-plane lattice thermal conductivities of multilayer graphene films. *Carbon* **2011**, *49*, 2653–2658. [CrossRef]
131. Cao, H. Molecular dynamics simulation study on heat transport in monolayer graphene sheet with various geometries. *J. Appl. Phys.* **2012**, *111*, 083528. [CrossRef]

132. Garg, A.; Vijayaraghavan, V.; Wong, C.H.; Tai, K.; Gao, L. An embedded simulation approach for modeling the thermal conductivity of 2D nanoscale material. *Simul. Model. Pract. Theory* **2014**, *44*, 1–13. [CrossRef]
133. Prabakaran, R.; Kumar, J.P.N.; Lal, D.M.; Selvam, C.; Harish, S. Constrained melting of graphene-based phase change nanocomposites inside a sphere. *J. Therm. Anal. Calorim.* **2020**, *139*, 941–952. [CrossRef]
134. Prabakaran, R.; Sidney, S.; Lal, D.M.; Selvam, C.; Harish, S. Solidification of Graphene-Assisted Phase ChangeNanocomposites inside a Sphere for ColdStorage Applications. *Energies* **2019**, *12*, 3473. [CrossRef]